Interactions of Ebolavirus proteins with the autophagy pathway

A thesis submitted to the University of Kent for the degree of

M.Sc. Microbiology in the Faculty of Science, Technology and Medical Studies

2018

Rebecca Steventon

School of Biosciences

I Declaration

No part of this thesis has been submitted in support of an application for any degree or qualification of the University of Kent or any other University or institute of learning.

Rebecca Steventon

August 2018

II Acknowledgements

I would like to thank my lab colleagues, Fred, Matt and Diego, who provided help with techniques and any questions I had throughout the project. I would like to thank Matt and Diego for their support with using the confocal microscope.

Mostly I would like to thank my supervisor Dr Jeremy Rossman, for providing knowledge and advice throughout the project and allowing me to complete this project within his laboratory.

III Contents

IV List of Figures

V List of Tables

VI Abbreviations

ATG	Autophagy Related Gene
CD4	Cluster of Differentiation 4
CD8	Cluster of Differentiation 8
DAPI	4,6-diamidino-2-phenylindole
DNA	Deoxyribonucleic acid
EBOV	Zaire Ebolavirus
EBSS	Earle’s Balanced Salt Solution
FIP200	FAK Family Interacting Protein of 200kB
GABARAP	Gamma-aminobutyric acid receptor-associated protein
GFP	Green Fluorescent Protein
GP	Glycoprotein
GTP	Guanosine Triphosphate
HA	Human Influenza Hemagglutinin
IFN-gamma	Interferon gamma
IgG	Immunoglobulin G
IL-12	Interleukin 12
IL-2	Interleukin 2
L	RNA Dependent RNA Polymerase
Lamp	Lysosome-associated membrane protein
LC3	Microtubule-associated protein 1 light chain
LIR	LC3 interacting region
M2	Matrix 2
MEF	Mouse Embryonic Fibroblast

mTORC1	Mammalian target of Rapamycin complex 1
NP	Nucleoprotein
NP-40	Nonyl Phenoxypolyethoxylethanol
PE	Phosphatidylethanolamine
PEI	Polyethylenimine
PI3K	Class III phosphatidylinositol-3-kinase
PSSM	Custom Position-Specific Scoring Matrix
ptdSer	Phosphatidylserine
Rab 7	Ras-related protein
RNA	Ribonucleic acid
SDP	Specificity Determining Position
TBS	Tris Buffered Saline
TBS-T	Tris Buffered Saline with Tween
TLR	Toll-Like Receptor
TNF	Tumour Necrosis Factor
TPC	Two-pore channels
trVLP	Transcription and replication virus like particle
ULK1	Serine/Threonine protein kinase
UVRAG	UV Irradiation resistance -associated tumour suppressor gene
VLP	Virus Like Particle
VP	Viral Protein

VII Abstract

Macroautophagy is a cellular process involved in maintaining cellular homeostasis. It plays a role in many viral infections, but the exact role it takes is highly viral and cellular specific. The role of macroautophagy in filoviridae infection is poorly understood. Ebolavirus is a member of the filoviridae family, along with Marburg virus. Previous scientific literature has shown that large Marburg nucleoprotein inclusions can induce the formation of LC3 puncta, which is indicative of the activation of autophagy, and that the autophagy protein LC3 is required for Ebolavirus entry. This project aimed to understand which Ebolavirus proteins could activate autophagy, and what effect they have on the overall autophagy pathway. Initially, bioinformatics was used to predict which proteins may be able to activate autophagy by determining potentially functional LIR domains present within Ebolavirus proteins. These results were then tested experimentally. These experiments identified three Ebolavirus proteins that could potentially activate autophagy, zNP, zVP35 and zVP40. The effect of these proteins on the overall autophagy pathway was then investigated, looking at the maturation stages of the autophagy pathway. The results from these experiments suggested that the autophagosomes undergo fusion with lysosomes, but autophagic flux is inhibited. A trVLP system was used to look at the role of autophagy on the replication and budding of Ebolavirus. Results show that autophagy may play a role in aiding viral replication, but hindering the budding of virus like particles. Overall, this study showed that EBOV proteins are able to interact with the autophagy pathway, and the autophagy pathway may play a vital role in the replication process of Ebolavirus.

1 Introduction

1.1 Ebolavirus

The first cases of haemorrhagic fever attributed to Ebolavirus were recorded in 1976. Since then Ebolavirus has been classified as belonging to the *Filoviridae* family, along with Marburg virus. Filoviruses are enveloped, non-segmented, negative sense RNA viruses with characteristic filamentous particles [Sanchez, A., 1993]. Within Ebolavirus viral particles, the single stranded negative sense RNA genome is of 19kb length [Mahanty, S., 2004]. The genome contains seven genes, arranged in the following fashion: 3'-NP-VP35-VP40-GP-VP30-VP24-L-5', as can be seen in Figure 1. Transcription of the genome begins at the 3' end [Sanchez, A., 1993]. Ebolavirus genes all encode single proteins, apart from GP, which encodes three separate proteins; glycoprotein (GP), soluble GP (sGP) and small soluble GP (ssGP) [Mehedi, M., 2011].

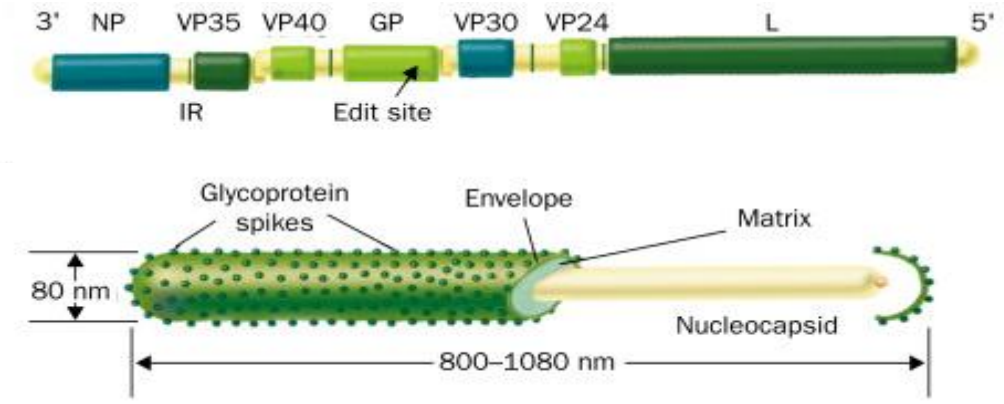

Figure 1: A schematic diagram of the Ebolavirus genome and filamentous particle.

Schematic diagram of the Ebolavirus genome from 3' to 5' end, showing the 7 main Ebolavirus proteins, with a schematic diagram of an Ebolavirus filamentous particle, showing GP on the surface [Mahanty,S., 2004]

All the Ebolavirus proteins play a part in the formation of new viral particles. GP is the only transmembrane surface protein, and forms trimeric spikes on filamentous particles, and is required for viral entry. The nucleoprotein (NP), VP30, VP35 and L all form part of the replication complex, with NP, VP30 and VP24 forming nucleocapsids around new genomes. VP40 is a matrix protein that is required for virion structural integrity as well as viral egress. Ebolavirus proteins also interact with the host immune response, with VP35 and VP24 both interacting with the interferon response of host cells [Mahanty,S., 2004].

1.1.1 Viral Spread

Ebolavirus outbreaks are mostly recorded in humans and great apes, with high infection rates in both species. These species are thought to act as accidental hosts for the virus, due to the high mortality rates of infection within the species [Pratt, W.D., 2010]. The reservoir species for Ebolavirus has not yet been identified, although it could be maintained in small mammals such as rodents or bats. Recent findings suggest African fruit bats may serve as a reservoir species after detection of viral nucleotide sequence was identified in three fruit bat species [Leroy, E.M., 2005]. However, the virus itself could not be isolated [Leroy, E.M., 2005].

Little is known about the nature of transmission of Ebolavirus from bats or other reservoir species to humans [Pratt, W.D., 2010]. However, the nature of transmission of Ebolavirus between humans is well understood. Ebolavirus can be easily transmitted via many bodily fluids such as saliva and blood during the acute period of infection [Bausch, D.G., 2007]. However, if correct infection controls are in place, the transmission of Ebolavirus via fomites is very rare [Bausch, D.G., 2007].

1.1.2 Symptoms of Ebolavirus Infection

Initial symptoms of Ebolavirus infection often appear flu like, with symptoms including fever, chills, and malaise [Feldmann,H., 2011]. As the infection persists, multi system involvement appears, with gastrointestinal, respiratory and systemic symptoms appearing such as vomiting, abdominal pain, cough and prostration [Feldmann,H., 2011]. Haemorrhagic manifestations arise during the peak of the illness and include petechiae and ecchymoses. Patients with fatal disease develop clinical signs early during infection and die typically due to multiorgan failure [Feldmann,H., 2011].

1.1.3 Clinical Manifestation

The initial target cells of Ebolavirus are dendritic cells and macrophages, as can be seen in Figure 2.

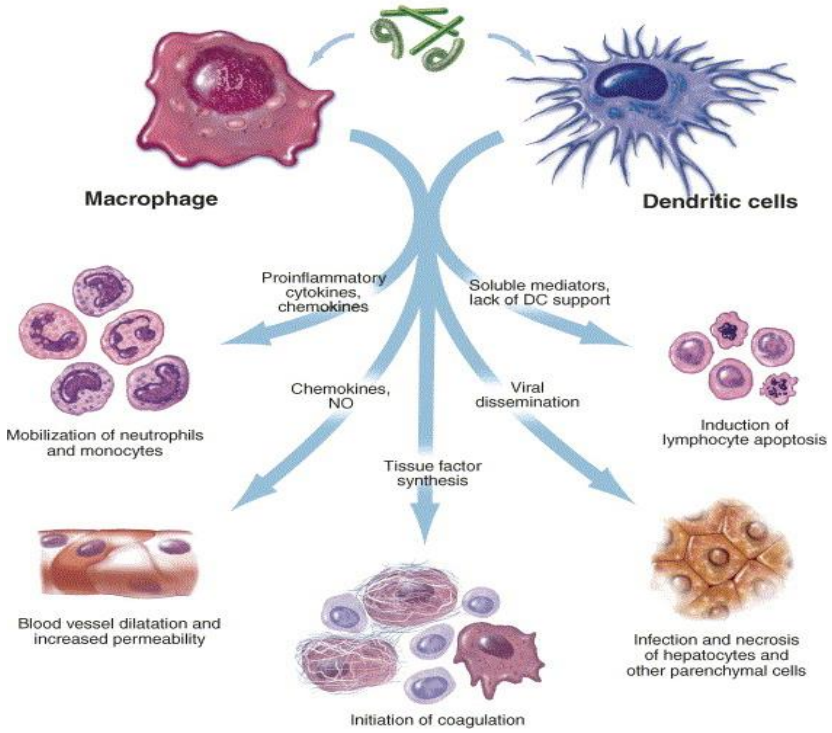

Figure 2: A schematic overview of Ebolavirus infection of human cells

A diagram to show the cells that Ebolavirus infects and the effect on the innate and adaptive immune system that infection has [Bray,M., 2005].

These cells aid in the dissemination of the virus as they carry the virus to regional lymph nodes where the virus can replicate. Free and monocyte associated virions can travel through lymphatic channels and the bloodstream to many different tissues such as the spleen and liver, as well as infecting other cell types such as parenchymal cells, endothelial cells, epithelial cells and hepatocytes. This ability to spread throughout the body and infect many different tissue and cell types leads to multi organ infection [Feldmann,H., 2011].

1.1.4 Immune Response

During Ebolavirus infection, a robust immune response is produced with the expression of many strong inflammatory mediators such as interleukins 2, 6, 8, and 10, TNFα; and reactive oxygen and nitrogen species [Feldmann,H., 2011]. Expression of these mediators results in an immune imbalance during infection which contributes to the progression of the disease.

Two Ebolavirus proteins can interfere with the interferon response during infection. VP35 acts as a type I interferon antagonist by possibly preventing transcription of interferon β as well as blocking activation of interferon regulatory factor 3 [Feldmann,H., 2011], while VP24 interferes with the type I interferon response by interacting with STAT1.

Reactive oxygen and nitrogen species play an important role during Ebolavirus infection. Nitric oxide when produced abnormally can result in tissue damage and loss of vascular integrity. Nitric oxide can also act as a mediator of hypotension, which is present during Ebolavirus infection [Feldmann,H., 2011]. EBOV induces abnormal levels of nitric oxide during infection which can lead to the apoptosis of lymphocytes. Lymphocyte apoptosis begins early in infection and can

also be caused by other mediators such as TNF-α, resulting in progressive lymphopenia throughout the course of infection [Bray,M., 2005]. During infection Ebolavirus can induce a robust immune response, which many of the symptoms of Ebolavirus can be attributed to.

1.2 Ebolavirus Species

Within the *Ebolavirus* genus, there are five different species; Zaire ebolavirus (EBOV), Reston ebolavirus (RESTV), Sudan ebolavirus, Tai Forest ebolavirus and Bundibugyo ebolavirus [Kuhn, J.H., 2010]. The first outbreak in 1976 was caused by the EBOV species and had a case fatality rate of 88%. Since then, there have been ten more outbreaks of Ebolaviruses which have been attributed to the EBOV species. EBOV has caused the most recorded outbreaks in humans, and has the highest mortality rate, with an average of 90% [Lefebvre, A., 2014].

Another species of Ebolavirus, RESTV, was first identified in 1989 in Reston, USA in cynomolgus monkeys which had been imported from the Philippines [Miranda, M.E., 1999]. The clinical symptoms of the monkeys infected with RESTV were diarrhoea, respiratory illness and haemorrhage, and the source facility saw a case fatality rate of 82% in the monkeys [Miranda, M.E.G., 2011].There have been two more RESTV outbreaks in nonhuman primates ; in 1992 in Sienna, Italy and in 1996 in the USA [Miranda, M.E.G., 2011], with all outbreaks being attributed to monkeys imported from the Philippines. During these three outbreaks, 458 people, who had some form of contact with the infected monkeys, were tested. Five samples came back seropositive for IgG antibodies to RESTV, showing a possibility for transmission between humans and monkeys [Miranda, M.E.G., 2011]. In

2008, RESTV was found in domestic pigs in the Philippines [Barrette, R.W., 2009]. There were 6 cases of humans being seropositive for IgG to RESTV [Barrette, R.W., 2009], showing that the virus can transmit from swine to human. However, in all cases of RESTV transmission to humans, there was no evidence of disease within humans, making RESTV the only Ebolavirus species to be non-pathogenic to humans [Miranda, M.E.G., 2011] [Barrette, R.W., 2009].

1.2.1 Pathogenicity of Different Species

The reason behind the difference in pathogenicity between RESTV and the other species of Ebolavirus is still unknown. All Ebolaviruses produce the same 9 proteins, but these proteins have been shown to contain amino acid changes which could account for the difference in pathogenicity. 189 Specificity Determining Positions, amino acids that are conserved between sub families, but differ between species, were determined between RESTV and pathogenic Ebolavirus [Pappaardo, M., 2016].

These amino acid changes could account for the different interactions that occur with cellular pathways seen between EBOV and RESTV. EBOV VP35 and VP24 counteract the IFN response within cells leading to upregulation of IFN genes, while during RESTV infection there is a minimal change in expression of IFN genes [Olejnik,J., 2017]. Another pathway targeted during EBOV infection is the expression of cytokines and chemokines via the upregulation of genes involved in NF-kB signalling. RESTV only moderately affects the expression of these genes [Olejnik,J., 2017].

1.3 Viral Replication

Another reason for the reduction in pathogenicity could be due to the process of viral replication. The genome cannot be transcribed by host cell enzymes, requiring all components for viral replication to be carried with the virion, or to be produced during viral infection, [Mahanty, S., 2004], with an overview of this process being seen in Figure 3.

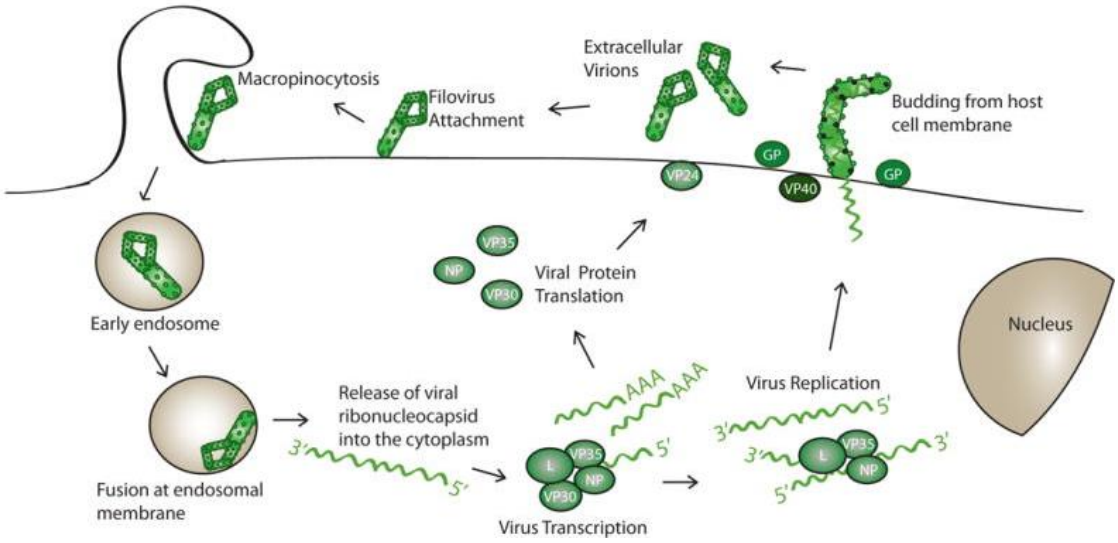

Figure 3: A schematic overview of the viral replication cycle of Ebolavirus. Entry occurs via macropinocytosis, then the virion is released into the cell before viral replication occurs, involving inclusion bodies formed of NP,VP30, VP35 and L.GP and VP40 are involved in virion release [Messaoudi,I., 2015]

Replication for Ebolavirus begins with entry of the virus into host cells. Ebolavirus is taken into host cells via the interaction of *N*- and *O*- linked glycans on GP with C-type lectins on the cell surface, as well as Phosphatidylserine (PtdSer) receptors on the cell surface interacting with PtdSer present in the viral envelope [Rhein, B.A., 2015]. C-type lectins are found on many different cell types such as macrophages and dendritic cells. This triggers a process known as

macropinocytosis, where the plasma membrane ruffles, allowing the virus to enter the cell. The virus enters the cell and is encapsulated in a macropinosome. The macropinosome then fuses with a Rab7 positive endosome, which causes the viral envelope to fuse with the cellular endosomal membrane, in a low pH, capthesin dependent manner [Nanbo, A., 2010]. Once fusion has occurred, the viral core is released into the cytoplasm.

Once released into the cytoplasm, the replication cycle of Ebolavirus can begin. The replication complex is made up of VP30, NP, VP35 and L. This complex generates mRNA transcripts and copies the genome to produce full length positive sense RNA antigenomes, which act as templates for genome synthesis [Mahanty, 2004]. NP, L, VP35 and VP24 form ribonucleoprotein complexes which can be found within nucleocapsids [Hoenen, T., 2012]. Nucleocapsids are rod-like filamentous particles which have a diameter of 50nm, and a 1000nm length. These nucleocapsids accumulate in viral inclusions bodies, which also contain NP, VP30, VP35 and L [Hoenen, T.,2012]. Inclusion bodies are located in the perinuclear region of the cell [Schudt, G., 2015], and these act as the site of viral replication.

After the viral components have been replicated, the nucleocapsids are transported to the plasma membrane via actin polymerisation [Schudt, G., 2015], which requires VP40 [Noda, T., 2006]. VP40 is essential for viral release from the cell, as during the late stages of viral egress, VP40 recruits host proteins via its L budding domains which are essential for cell release [Han, Z., 2017]. Filamentous particles, containing nucleocapsids, are produced at the cell membrane [Noda, T., 2006]. Filamentous particles can vary greatly in length but have a uniform diameter

of 80nm [Sanchez, A., 1993]. Virions bud from the cell as filamentous virions in a vertical manner [Noda, T., 2006].

RESTV and EBOV both follow this viral replication route. However, there has been some evidence that viral replication occurs less efficiently in RESTV compared to EBOV, but the cause of this difference is still yet to be determined [Boehmann, Y., 2005].

1.4 Cell Death Pathways

As previously mentioned, during EBOV infection, lymphocytes undergo apoptosis [Bray,M., 2005]. Apoptosis is one of the cell death pathways that can be activated during viral infection, along with necrosis, and autophagy. Cell death pathways are activated during viral infection as a defence mechanism by the cells to prevent viral replication and spread. However, sometimes these pathways can aid the virus, as seen with lymphocyte apoptosis in EBOV infection. Lymphocyte apoptosis in EBOV infection suppresses the adaptive immune response produced by the host, allowing EBOV to replicate and disseminate throughout the body, leading to a fatal outcome for the host [Wauquier,N., 2010]. The role of other cell death pathways, such as autophagy, during EBOV infection are more poorly understood.

1.5 Basic Autophagy

Autophagy is a cellular process involved in maintaining cellular homeostasis, during which cellular content is degraded via a 'self-digestion' process [Wong,A.S.L., 2011]. There are three different forms of autophagy, which are defined by the way the cellular content is directed for degradation; chaperone-mediated autophagy, microautophagy and macroautophagy [Chiramel,A.I., 2013]. Macroautophagy, referred to as autophagy for the duration of this report, involves the formation of a

phagophore, that evolves into a double membraned vesicle called an autophagosome [Chiramel,A.,I., 2013]. The autophagosomes surrounds the cellular contents intended for degradation [Hosokawa,N., 2009].]. Once formed, the autophagosome can either fuse with a lysosome to form an autolysosome [Hosokawa, N.,2009] or fuse with an endosome to form an amphisome [Chiramel, A.I., 2013]. After fusion, degradation of the cellular contents of the autophagosome occurs. This pathway can be seen in Figure 4.

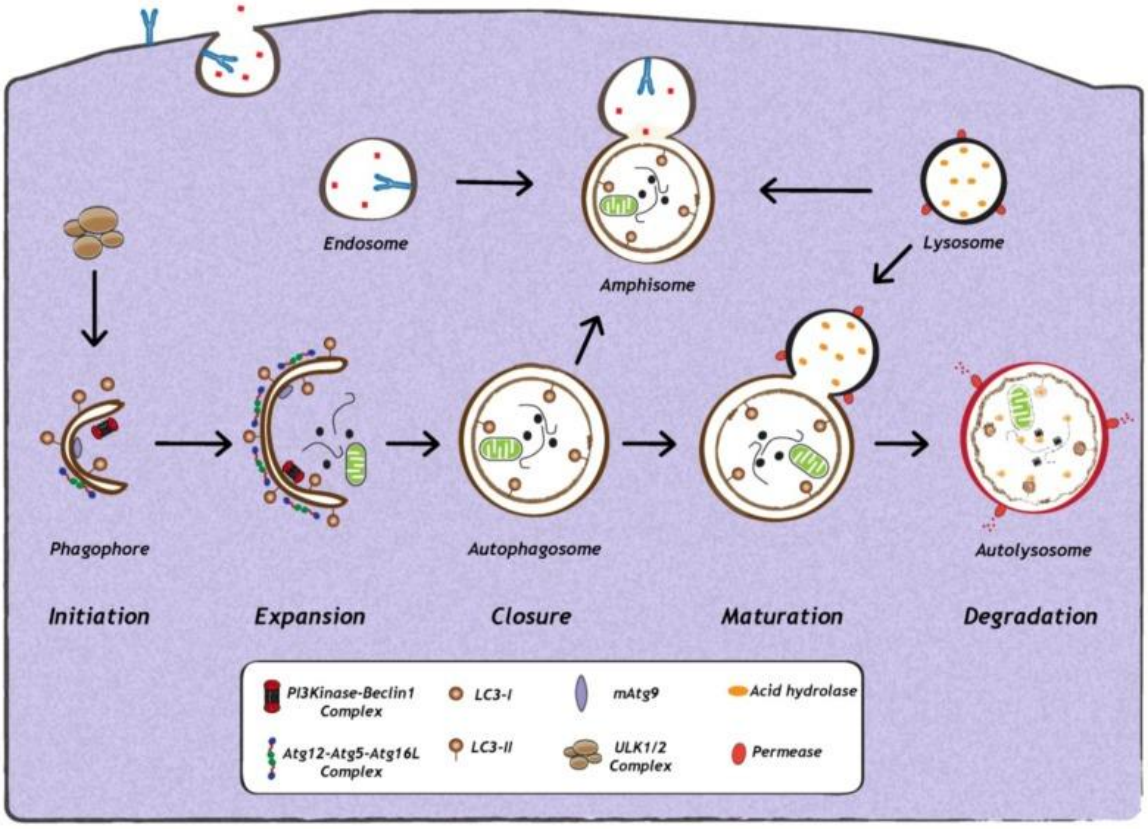

Figure 4: A schematic diagram to show the basic pathway of autophagy. Following initiation, a phagophore is created. This then expands to form an autophagosome. The autophagosome can then either fuse with a lysosome or endosome, resulting in degradation of the cellular contents of the autophagosome [Chiramel,A.,I., (2013)].

Autophagy can be induced via starvation to provide nutrients for the cell, during which non-specific methods are used to take up bulk cytoplasm resulting in the degradation of cytoplasmic content [Jager, S.,2004]. However, autophagy can also be activated and can selectively take up proteins, organelles, and intracellular pathogens [Wong, A.S.L., 2011], such as via the LC3 interacting protein p62. p62 binds poly- and mono-ubiquitin proteins via its ubiquitin associated domain [He, C., 2009], but can also bind LC3 via its LC3 interacting region (LIR) [Ichimura, Y., 2010]. This allows p62 to link its ubiquitinated cargos to autophagy machinery for autophagic degradation [He, C., 2009].

1.6 Autophagy Pathway

The initiation of autophagy requires the ULK complex [Wong,A.S.L., 2011], which consists of Atg13, ULK1 and FIP200 [Hosokawa,N.,2009].This complex is highly regulated via mTORC1, which can directly bind to the complex during high nutrient levels and prevent initiation of autophagy [Hosokawa,N., 2009]. Once initiated, the autophagy pathway begins with the formation of a flattened membrane sac called an isolation membrane or phagophore [Hosokawa,N.,2009]. The isolation membrane then undergoes elongation and nucleation to form vesicular structures; autophagosomes. Nucleation requires the formation of the PI3K/Beclin-1 complex, which is stimulated via the binding of UVRAG [Wong,A.S.L., 2011]. Following nucleation, elongation and expansion of the isolation membrane occurs via the binding of Atg proteins [Wong,A.S.L., 2011]. Atg5 forms a conjugate with Atg12 via an ubiquitination reaction involving Atg7 and Atg10 [Fujita,N., 2008]. This conjugate is essential for the elongation of the isolation membranes.

LC3-I is normally evenly distributed throughout the cytosol but becomes lipidated during autophagy to LC3-II, and localises to the inner and outer membranes of autophagosomes [Chiramel,A.I., 2013]. LC3-I forms an intermediate with Atg3 which is then activated via Atg7. This intermediate is then recruited to the isolation membrane via an interaction between Atg3 and Atg12. Once the Atg-LC3 intermediate is in the proximity of the isolation membrane, LC3 can undergo ubiquitination reactions with PE, which leads to the lipidation of LC3-I to LC3-II [Fujita,N., 2008].

Following elongation and closure of the isolation membrane to form the autophagosome, the autophagosomes fuse with early or late endosomes as well as lysosomes during autophagosomal maturation. Rab7 is a GTP binding protein required for the fusion of autophagosomes with endosomes and then lysosomes allowing the degradation of the cytosolic contents of the autophagosome [Jager,S., 2004].

1.7 LIR's

LIR's are LC3 interacting regions, a term coined by Pankiv and colleagues regarding the 22-residue peptide present in p62 that recognises LC3 [Kalvari, I., 2014]. This was shortened to a stretch of 11 conserved acidic and hydrophobic residues that act as the interacting region for mouse p62-LC3. When structural data became available for the interaction between human p62-LC3 the interacting region was pinpointed to a tetrapeptide sequence of WxxL, with x standing for any residue. The tryptophan and leucine residues interact with hydrophobic pockets of LC3 [Kalvari, I., 2014]. A sequence was determined by Alemu and colleagues, using 26 experimentally determined LC3 interacting regions. The typical sequence

pattern, [DE][DEST][**WFY**][DELIV]X[**ILIV**], carries through the **W**xx**L** motif [Alemu, E.A.,2012]. The newest consensus sequence is [ADEFGLPRSK] [DEGMSTV][**WFY**][DEILQTV] [ADEFHIKLMPSTV][**ILV**] [Jacomin, A-C., 2017]. LIRs allow proteins to interact with LC3, and this allows proteins either to be taken into autophagosomes to be degraded, or to affect autophagy in some way. Kalvari, and colleagues developed a computational approach to identifying these potential LIR domains using the consensus sequence. We previously determined the potential LIR domains of Ebolavirus, using the iLIR website (https://ilir.warwick.ac.uk/), with meaningful results being stated as results with PSSM scores of greater than 10. The PSSM score is an L x 20 scoring matrix with each element representing a log-odds score for the presence of a residue in the respective position [Kalvari, I., 2014] Recently, Jacomin, and colleagues adapted the LIR website, to be specific for viruses, although there is currently only one LIR dependent interaction that has been reported, that of the M2 protein of the Influenza A virus [Jacomin,A-C., 2017][Beale,R.,2014].

1.8 Role in Viral Infection

Autophagy can be induced during a viral infection, but the autophagy response to a viral infection is highly viral and cellular specific. Autophagy can act as an anti-viral defence mechanism, with viral components being taken into autophagosomes and then degraded. Autophagy can also aid in the activation of the innate immune system by exposing pathogen-associated molecular patterns to innate immune sensors via viral components being taken up into autophagosomes, and these fusing with endosomes [Sparrer, K.M.J., 2018]. HIV-1 and HSV-1 are examples of viruses that are sensitive to viral clearance by autophagy [Sparrer,

K.M.J., 2018]. On the other hand, viruses like Zika virus and Influenza virus can subvert autophagy, using it to promote viral replication [Sparrer, K.M.J., 2018].

1.8.1 Role in Ebola Infection

The role of autophagy during filoviridae viral infection is poorly understood. Marburg virus and Ebolavirus both produce nucleocapsids utilizing the same viral proteins, and viral RNA synthesis occurs in inclusion bodies for both viruses [Dolnik, O.,2015]. Dolnik et al (2015) showed that during Marburg virus infection, LAMP1 can be detected in VP40 clusters and in NP inclusions containing VP40, suggesting an interaction between LAMP1 and VP40 and its recruitment into inclusion bodies [Dolnik,O., 2015]. LC3 positive puncta were also detected in larger NP inclusions formed during Marburg virus infection, as can be seen in Figure 5 [Dolnik, O.,2015]. These results suggest a regulation of autophagy during Marburg virus infection, and that this regulation could be associated with viral inclusion bodies.

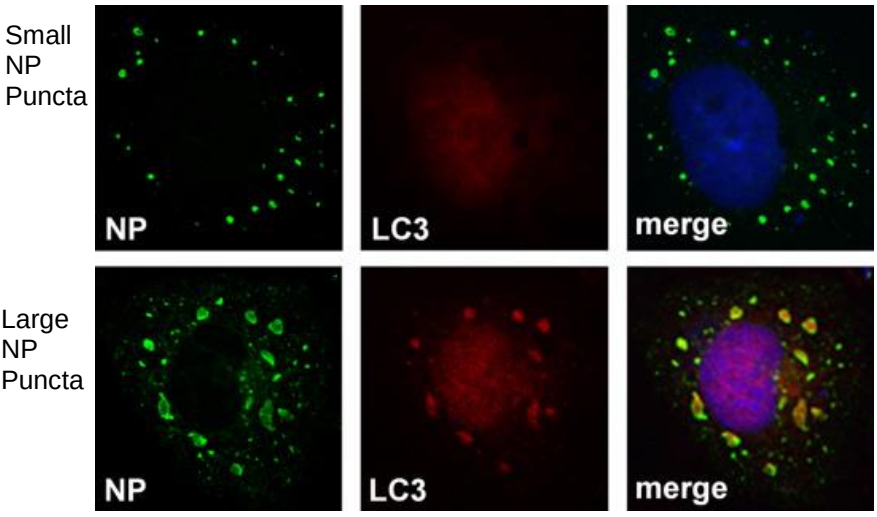

Figure 5: Large NP inclusions co-localised with LC3 during Marburg virus infection in huh-7 cells.

MEF cells were transfected with Marburg NP and LC3. The presence of LC3 puncta colocalising with NP was observed with large NP puncta [Dolnik,O., 2015].

FAM134 is part of the reticulon protein family and is an ER- resident receptor that can bind to autophagy modifiers LC3 and GABARAP [Khaminets, A., 2015]. Via its ability to bind to autophagy modifiers, FAM134 can control endoplasmic reticulum turnover via selective autophagy [Khaminets, A., 2015]. In a 2016 paper written by Chiramel, it was found that a specific FAM134, FAM134B, inhibits replication of Ebolavirus strains Makona and Mayinga, strains which belong to the EBOV species. When FAM134B is missing from cells, there are increased levels of viral replication, as well as increased expression of multiple viral proteins, increased inclusion body formation and greater production of infectious virus [Chiramel, A.I., 2016]. This shows that the turnover of the ER by autophagy is an important limiting factor to Ebolavirus replication. However, this paper does not show the effect of macroautophagy on Ebolavirus replication, instead showing that if there is a greater amount of ER present within the cell, then this allows for more general viral protein translation, not what effect the autophagy is having on the virus [Chiramel, A.I., 2016].

A recent paper showed that the autophagy protein LC3 is required for EBOV internalisation into cells [Shtanke,O. 2018]. LC3B has been seen to associate with mature macropinosomes, suggesting that autophagy proteins may play a role in macropinocytosis; the entry method used by EBOV. The paper showed that LC3-I and LC3-II both associate with macropinosomes, but LC3-II is required for vesicle internalisation from the cell surface [Shtanke,O., 2018]. The paper also showed that EBOV associated with the macropinsomes that LC3 was interacting with. Overall, the paper shows that autophagy proteins, specifically LC3 -II, are required for EBOV internalisation into the cell after binding via GP [Shtanke,O., 2018].

Our preliminary work showed that NP may be able to activate autophagy when transfected within Mouse Embryonic Fibroblasts (MEF) cells. The presence of LC3 puncta, which are indicative of autophagosomes, and increased levels of LC3-II, were seen and are shown in Figure 6. However, this work did not look at the full genome of EBOV to determine if NP is the only EBOV protein to activate autophagy, and whether this activation was having a pro-viral or anti-viral effect.

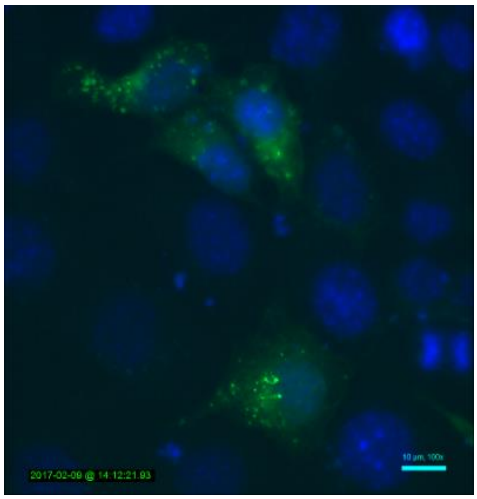

Figure 6: Induction of autophagy by zNP expression

Previously, LC3 puncta were seen in MEF cells transfected with GFP-LC3 and EBOV NP. LC3 puncta are seen as green, while nuclei were stained blue with DAPI.

1.9 Aims of the Project

The aims of this project were to determine which Ebolavirus proteins can activate autophagy, and the impact this has on viral replication. Firstly, the LIR domains present within the Ebolavirus proteins, that can activate autophagy, were determined. This was done by using the updated viral LIR web resource. Second, we looked for the presence of LC3 puncta within two cell lines, the previously used MEF cell line and a human cell line, HeLa, to determine the activation of autophagy by EBOV proteins. The next aim was to determine what effect the EBOV proteins were having on the maturation of the autophagy pathway. This was achieved by looking at the co-localisation of the EBOV protein with LAMP1 and LC3, and the

degradation of p62, an autophagic flux marker. The final aim of this project was to determine the effect autophagy has on the replication and budding of EBOV, by using a transcription and replication Virus Like Particle (trVLP) system in a wild type Hela cell line and HeLa's which are deficient in autophagy (HeLa-Hex).

2 Materials and Methods

2.1 Mammalian Cell Lines

Mouse Embryonic Fibroblasts, referred to as MEFs for this report, and HeLa cells were obtained from the Rossman laboratory. HeLa-Hex cells, containing CRISPR knock-outs of the eight Atg8 (LC3) family members were kindly provided by Michael Lazarou [Nguyen,T,N., 2016].

2.2 Tissue Culture

Cells were grown in Dulbecco's Modified Eagle Medium (DMEM) (PAN BioTech, UK) supplemented with 10% fetal bovine serum and 50ug/ml penicillin/streptomycin (Fisher Scientific). Cells were grown at 37^0c with 5% CO_2. Cells were grown to confluency before being passaged, usually every 3-5 days.

2.3 Plasmid Preparation

Plasmids for each Ebolavirus protein were obtained from the US-NIAID BEI resource facility. Each PCAGGS plasmid confers resistance against ampicillin and expresses one single Ebolavirus protein. All EBOV plasmid proteins are tagged with a HA tag, apart from GP. EBOV trVLP plasmids (pCAGGS-NP, pCAGGS-VP35, pCAGGS-VP30, pCAGGS-L, pCAGGS-T7, tetrascistronic minigenome, pCAGGS-Tim1) were kindly provided by Thomas Hoenen [Watt,A., 2014]. EGFP-LC3 was a gift from Karla Kirkegaard (Addgene plasmid #11546). pLamp1-mCherry was a gift from Amy Palmer (Addgene plasmid #45147).

2.4 Plasmid Transfections

Transfection of plasmids was carried out using PEI Transfection reagent (Polysciences). 1.5ug of plasmid was added to 100ul of Na-Cl. PEI transfection reagent was then added in a 4:1 PEI:DNA ratio. The complex was then vortexed for 5 seconds before incubating at room temperature for 10 minutes. The cell media was changed to an antibiotic free media, before 100ul of complex was added to the cells. Four hours later, the media was changed to antibiotic containing DMEM.

2.5 Antibodies

Primary antibodies used were: anti- HA-probe (F-7) sc-7392, (Santa Cruz Biotechnology), anti-Ebolavirus GP, clone 15H10, NR-12184 (BEI Resources), anti-SQSTM1/ p62 ab56416 (Abcam),

2.6 Fluorescence Microscopy Analysis – Panel

Cells were grown in 12-well plates on glass coverslips. At 80% confluency, the cells were transfected with viral protein expressing plasmid. After 24 hours, cells were washed with TBS twice and fixed using 10% formalin for 30 minutes. Cells were then permeabilized with 0.1% Triton X-100. After washing with TBS twice, blocking solution (1% BSA and 0.05% Tween20 in TBS) was added for 20 minutes. After washing with TBS, cells were incubated with primary antibody (anti-HA, or anti-GP). Primary antibody was prepared at the recommended dilutions with blocking solution. Primary antibody was incubated on the coverslip for one and a half hours at room temperature. Secondary antibody (Alexa Fluor 594 donkey anti-mouse) was diluted at the recommended levels in blocking solution. This was

stored in darkness to prevent fluorescence bleaching. After aspirating off the primary antibody, the slides were washed three times in TBS before secondary antibody was added. Secondary antibody was incubated for one hour at room temperature. Secondary antibody was aspirated, and the cells were washed three times with TBS. Cells were stained with Hoechst33342 for nuclear staining for 20 minutes. Cells were washed three times with TBS before being blotted dry. Cells were mounted using Prolong Gold Antifade reagent (ThermoFisher Scientific). Slides were left to dry for ~16 hours before being visualised using a Zeiss confocal microscope. Appropriate lasers and filters were used to visualise the different stains using a 100x objective. Zen black was used to export the images.

2.7 Fluorescence Microscopy Analysis – Maturation

Cells were grown and processed as above with the exception that cells were transfected at 70% confluency with viral protein expressing plasmids eGFP-LC3 and Lamp1 mCherry expressing plasmids. After 48 hours, cells were processed, stained with anti-HA and Alexa Fluor 680 donkey anti-mouse secondary antibody and imaged as above.

2.8 Western Blot Analysis

Cells were plated in a 12-well plate. When they reached 70% confluency, they were transfected with viral protein expressing plasmid. After 42 hours, EBSS and chloroquine (50μM) were added as positive controls. After 48 hours, cells were lysed using NP-40 lysis buffer containing Complete Mini protease inhibitor. Lysates were then centrifuged at 13, 300 rpm for 10 minutes and the supernatants were collected. Samples were separated using a Bio-Rad Criterion TGX Stain-Free Any

kD precast gel which was run for 60 minutes at 120V. The gels were transferred to a Polyvinylidene difluoride membrane using the Bio-Rad Trans-Blot Turbo Transfer System. The membranes were blocked using 5% w/v milk in 0.1% Tween20/TBS and incubated overnight in primary antibodies diluted in TBS-T. Horseradish peroxidase-conjugated donkey anti-mouse secondary antibody was then applied for an hour, before applying enhanced chemiluminescence reagents 1 and 2 (Bio-Rad) in a 1:1 ratio, to the blot. Visualisation was done using a SynGene G: Box using the GeneSys system for automatic imaging, and the processed using ImageJ for band intensity.

2.9 trVLP system

Producer cells were grown in a 6 well dish. At 50% confluency, the cells were transfected with 125ng pCAGGS-VP35, 75ng pCAGGS-VP30, 1000ng pCAGGS-L, 250ng tetracistronic minigenome expression plasmid, 250ng pCAGGS-T7 and 125ng pCAGGS-NP as previously described [Watt,A., 2014]. 72 hours later, the trVLP-containing supernatant of the p0 producer cells was clarified by centrifugation for 5 minutes at 800xg, room temperature. 1.5ml of the clarified supernatant was transferred onto p1 cells that had 24 hours previously been transfected with 125ng pCAGGS-NP, 125ng pCAGGS-VP35, 75ng pCAGGS-VP30, 1000ng pCAGGS-L, and 250ng pCAGGS-Tim1. p0 cells were then lysed using NP-40 lysis buffer with Complete Mini Protease Inhibitor. 30 minutes later, cells were resuspended in the lysis buffer. Lysates were then clarified by centrifugation for 10 minutes at 13,000rpm. 40ul of lysate was then added to 40ul RenillaGlo substrate in white 96 well plates. After incubation for 10 minutes, Renilla luciferase reporter activity was measured using a CLARIOstar plate reader. 72

hours later, p1 cells were lysed using NP-40 lysis buffer with Complete Mini Protease Inhibitor. 30 minutes later, cells were resuspended in the lysis buffer. Clarified lysates luciferase reporter activity was then measured.

2.10 Determination of LIR domains

Using the iLIR viruses website (http://ilir.uk/virus/), the potential LIR domains in all Zaire (Mayinga strain 76) proteins and all Reston (Reston strain 89) proteins were determined using the Search tool available on the website. To determine which of these potential LIR domains are most likely to be functional, the PSSM score of each protein was identified. PSSM scores between 9 and 18 were validated for their accuracy, sensitivity, and specificity. PSSM scores that lie between 13 and 17 were concluded to be meaningful values from this due to the levels of specificity and sensitivity [Kalvari, I., 2014]. However, when experimentally determined LIR domains were tested, PSSM scores as low as 7 were shown in functional LIR domains. Due to these experimentally determined LIR's PSSM scores, and the specificity and sensitivity of the PSSM scores, a PSSM score of 11 was used to determine potential LIR domains present in Zaire and Reston Ebolaviruses.

3 Results

3.1 Determination of Potential LIR domains

The aim of this experiment was to determine which EBOV proteins might interact with the autophagy pathway by looking for the presence of LIR domains within each EBOV protein sequence. To determine the domains most likely to encode functional LIR domains, the PSSM score is used as a measurement. Results show that zVP35 contains the most likely functional LIR domain (Table 1), with a total of 9 meaningful potential LIR domains across all the EBOV proteins (Table 1).

Protein	Start	End	LIR sequence	PSSM Score
zVP35	322	327	RGWVCV	16
zL	290	295	DGYKII	13
zL	424	429	GSWYSV	13
zL	714	719	KLWTSI	13
zVP40	93	98	PIWLPL	13
zL	492	497	TCWDAV	12
zL	1116	1121	YSWAHI	12
zNP	189	194	TAWQSV	12
zVP40	245	250	QDFKIV	11

Table 1: Meaningful potential LIR domains in EBOV proteins

LIR domains that satisfy certain criteria were ordered per PSSM score.

The same criteria were applied to the potential LIR domains in RESTV. Overall, there are more meaningful potential LIR domains present in RESTV compared to EBOV (Table 2). Many of these LIR domains have higher PSSM scores compared to their EBOV counterparts, apart from rVP40 (Table 2). rVP35 still contains the most likely functional LIR domain (Table 2).

Protein	Start	End	LIR Sequence	PSSM Score
rVP35	311	316	RGWVCL	17
rL	177	182	DEFIDI	14
rNP	599	604	PDYTAV	14
rGP	21	26	LVWVII	14
rL	424	429	GTWYSV	13
rL	714	719	KLWTSI	13
rL	1116	1121	YTWSHI	13
rVP40	93	98	PIWLPL	13
rL	349	354	RDFHKI	12
rL	492	497	TCWDAV	12
rNP	189	194	TAWQSV	12
rGP	3	8	SGYQLL	12
rL	290	295	EGYKII	11
rL	894	899	LDYGTI	11
rNP	19	24	LDYHKI	11
rNP	729	734	DKFLAI	11

Table 2: Meaningful potential LIR domains in RESTV proteins

LIR domains that satisfy certain criteria were ordered by PSSM score

To try and determine why the difference in LIR domains occurs between RESTV and EBOV, SDP's were cross referenced against the meaningful potential LIR domains of RESTV. SDP's can have four different effects on the LIRs of RESTV compared to EBOV LIR's; the LIR could disappear due to the SDP, a new LIR could appear due to the SDP, the PSSM score of the LIR could be affected due to the SDP, or there could be no effect on the LIR. There are five meaningful potential LIR domains in RESTV that overlap with an SDP region (Table 3).

Protein	Start	End	LIR Sequence	PSSM Score	Effect
rNP	599	604	PDYTAV	14	New
rL	1116	1121	YTWSHI	13	PSSM increase
rL	349	354	RDFHKI	12	New
rGP	3	8	SGYQLL	12	New
rL	894	899	LDYGTI	11	PSSM increase

Table 3: Meaningful potential LIR domains in RESTV proteins that overlap with a SDP

LIR domains that overlap with an SDP region in RESTV are listed, ordered by their PSSM scores. The SDP within the LIR sequence is highlighted in red.

These results suggest that both EBOV and RESTV contain LIR domains, and specific proteins will be able to interact with the autophagy pathway, although RESTV is predicated to contain more, and stronger domains.

3.2 Optimization of PEI Transfection

Evaluation of the optimal amount of plasmid for transfection was tested using titrations of 0.5ug, 1.0ug, 1.5ug and 2.0ug zNP in HeLa cells grown on glass coverslips. 24 hours post transfection, cells were fixed and stained for HA, and imaged by epifluorescence microscopy (Figure 7). Optimal amount of plasmid was determined to be 1.5ug due to transfection efficiency, NP puncta formation and cell viability.

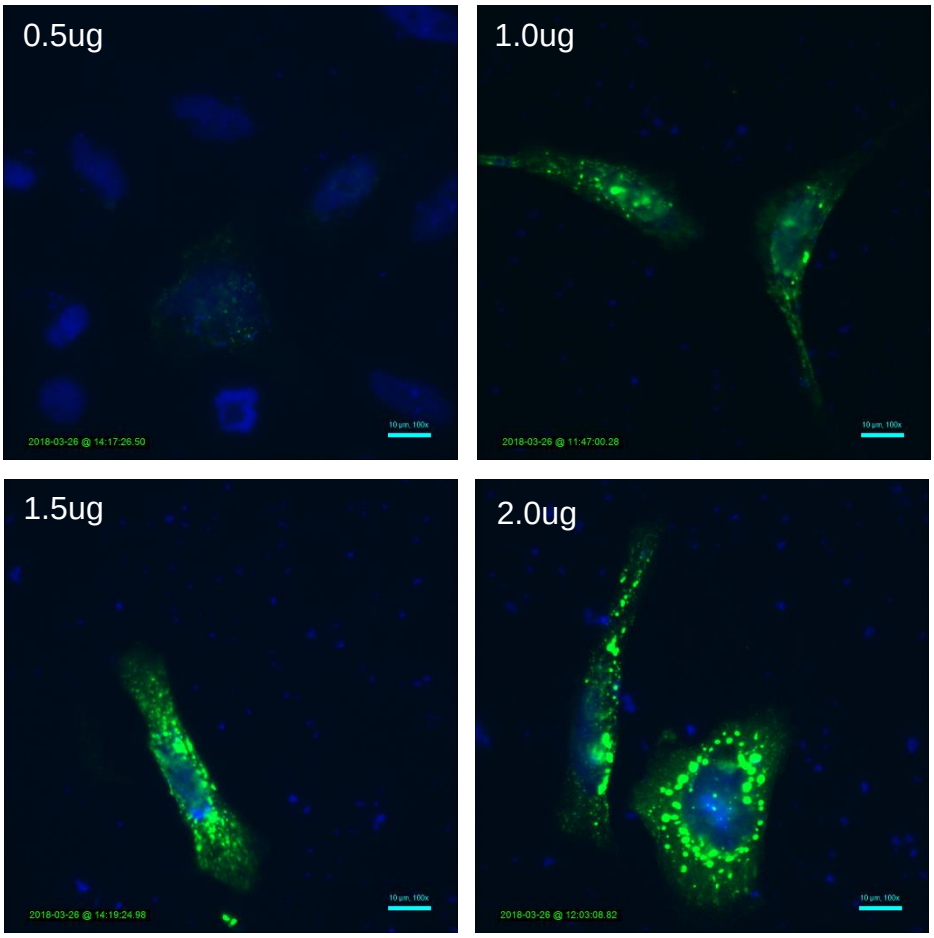

Figure 7:Optimization of PEI Transfection in HeLa cells

HeLa cells were transfected with varying amounts of zNP, as indicated besides the images. All slides were fixed and stained for NP (green), with nuclei being stained with DAPI (blue), 24hrs post transfection and analysed by fluorescence microscopy.

3.3 Induction of Autophagy by specific EBOV proteins

To get a comprehensive look at how EBOV may interact with autophagy, all EBOV proteins were tested for induction of autophagy. Firstly, MEF cells were transfected with individual EBOV protein expression plasmids, then 24 hours later, fixed, and imaged via fluorescence confocal microscopy (Figure 8). When there is little or no induction of autophagy in a cell, LC3 is seen evenly distributed throughout the cytosol, but during induction of autophagy, LC3 is redistributed to autophagosomes and this is seen as bright puncta. To get an idea of the basal level of autophagy in the cells, a negative control transfection of the empty vector plasmid pCAGGs was run. In the negative control, LC3 can be seen to be evenly distributed throughout the cell with only very small bright puncta formation, indicating the steady state levels of autophagy (Figure 8 and 9). zNP expression causes the greatest induction of autophagy of the EBOV proteins with numerous puncta formation, and puncta being distributed throughout the cytosol (Figure 8). zVP35 and zVP40 both also caused the formation of a few small puncta, which were close to the nucleus and distributed throughout the cytosol respectively (Figure 8). zVP30 also caused the formation of a few small puncta, which are located within the cytosol (Figure 8). This test was then re-run in human HeLa cells (Figure 9). Again, zNP, zVP35 and zVP40 all showed induction of autophagy with puncta being distributed evenly throughout the cytosol (Figure 9), but zVP30 showed no induction of autophagy (Figure 9).

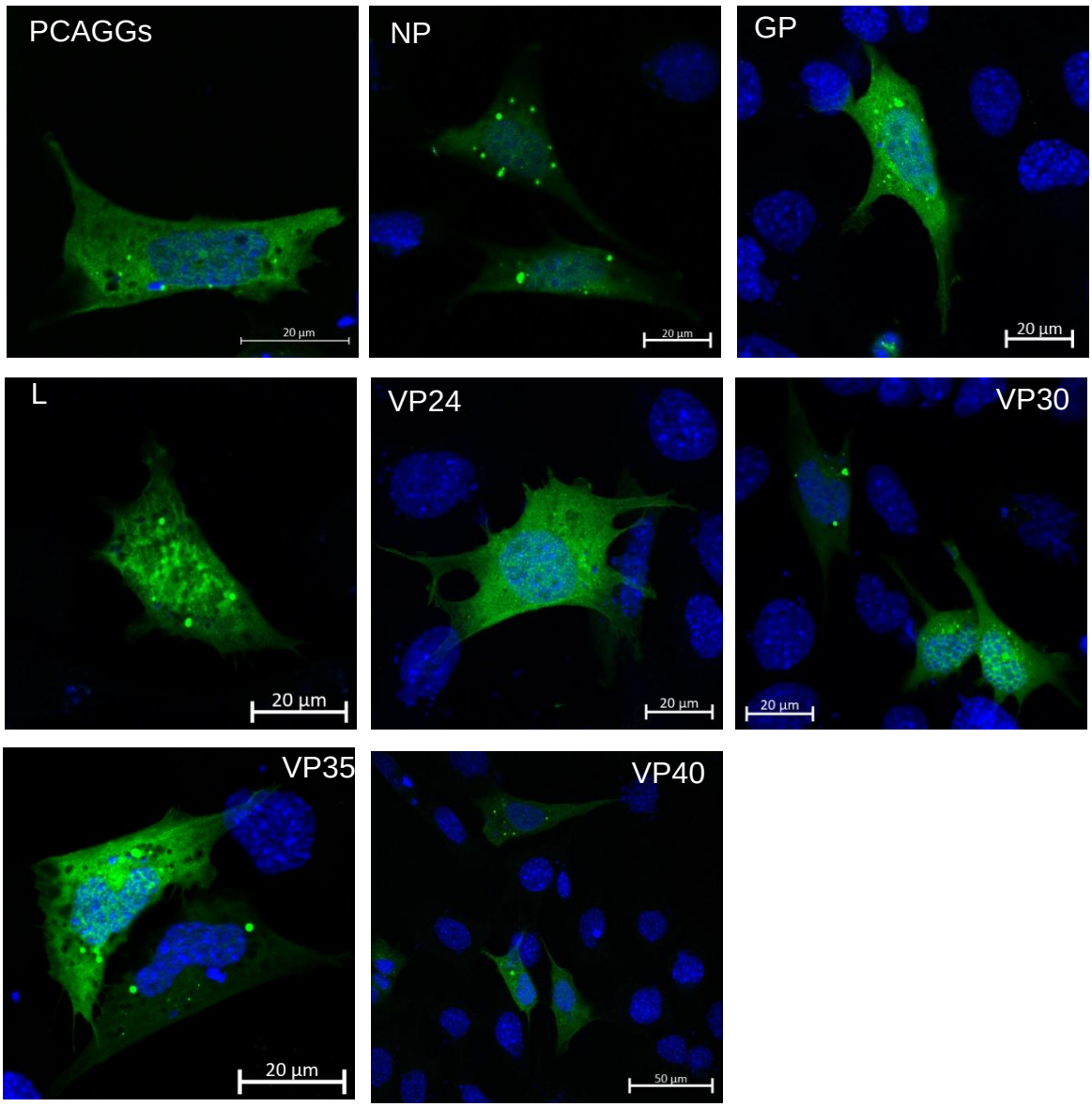

Figure 8: Specific EBOV proteins activate autophagy in MEF cells

MEF cells were transfected with individual EBOV proteins, as indicated besides the images, and GFP-LC3. Activation of autophagy is seen by the formation of LC3 puncta. LC3 puncta can be seen as bright green dots, or aggregations. All slides were fixed at 24hrs post transfection and analysed by confocal microscopy. Nuclei are stained blue by Hoechst33342.

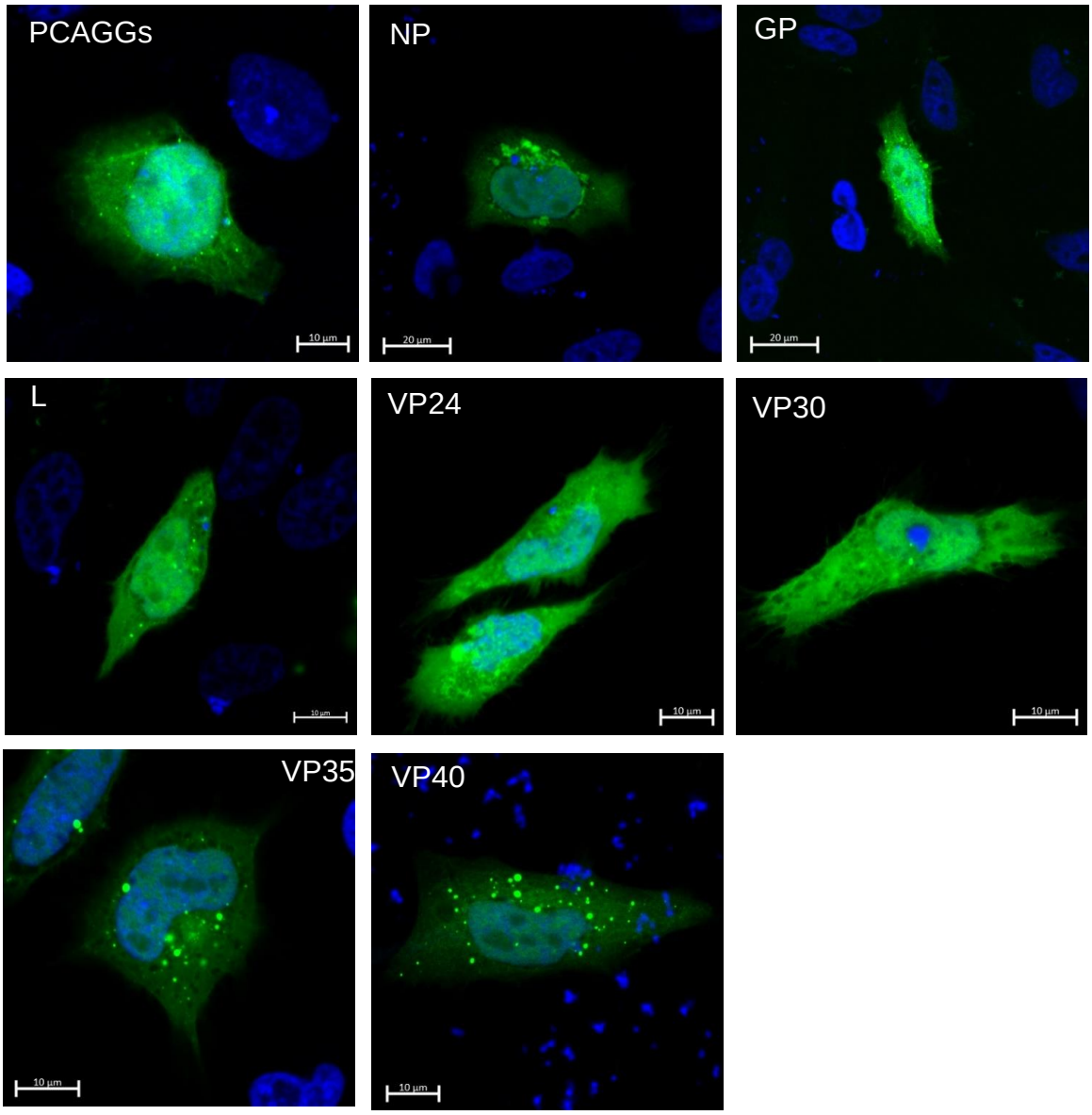

Figure 9: Specific EBOV proteins activate autophagy in HeLa cells

HeLa cells were transfected with individual EBOV proteins, as indicated besides the images, and GFP-LC3. Activation of autophagy is seen by the formation of LC3 puncta. LC3 puncta can be seen as bright green dots, or aggregations. All slides were fixed at 24hrs post transfection and analysed by confocal microscopy. Nuclei are stained blue by Hoechst33342.

3.4 Co-localisation of EBOV proteins with LC3 puncta

Whether the proteins are interacting with the autophagosomes or are just activating the autophagy pathway is an important distinction to determine. Co-localisation of the EBOV proteins and LC3 puncta was used to determine this. The three EBOV protein expression plasmids previously seen to activate autophagy were transfected into HeLa cells along with eGFP-LC3. 24 hours later, the cells were then fixed, and stained for the HA expression tag, before being imaged by confocal microscopy. zNP and GFP-LC3 are seen to co-localise with the formation of large aggregates containing both zNP and LC3 (Figure 10). zVP35 also appears to co-localise with LC3, with some of the LC3 puncta also being positive for the presence of zVP35 (Figure 10). However, there are some LC3 puncta that do not co-localise with zVP35. Only a few LC3 puncta appear to co-localise with zVP40 (Figure 10).

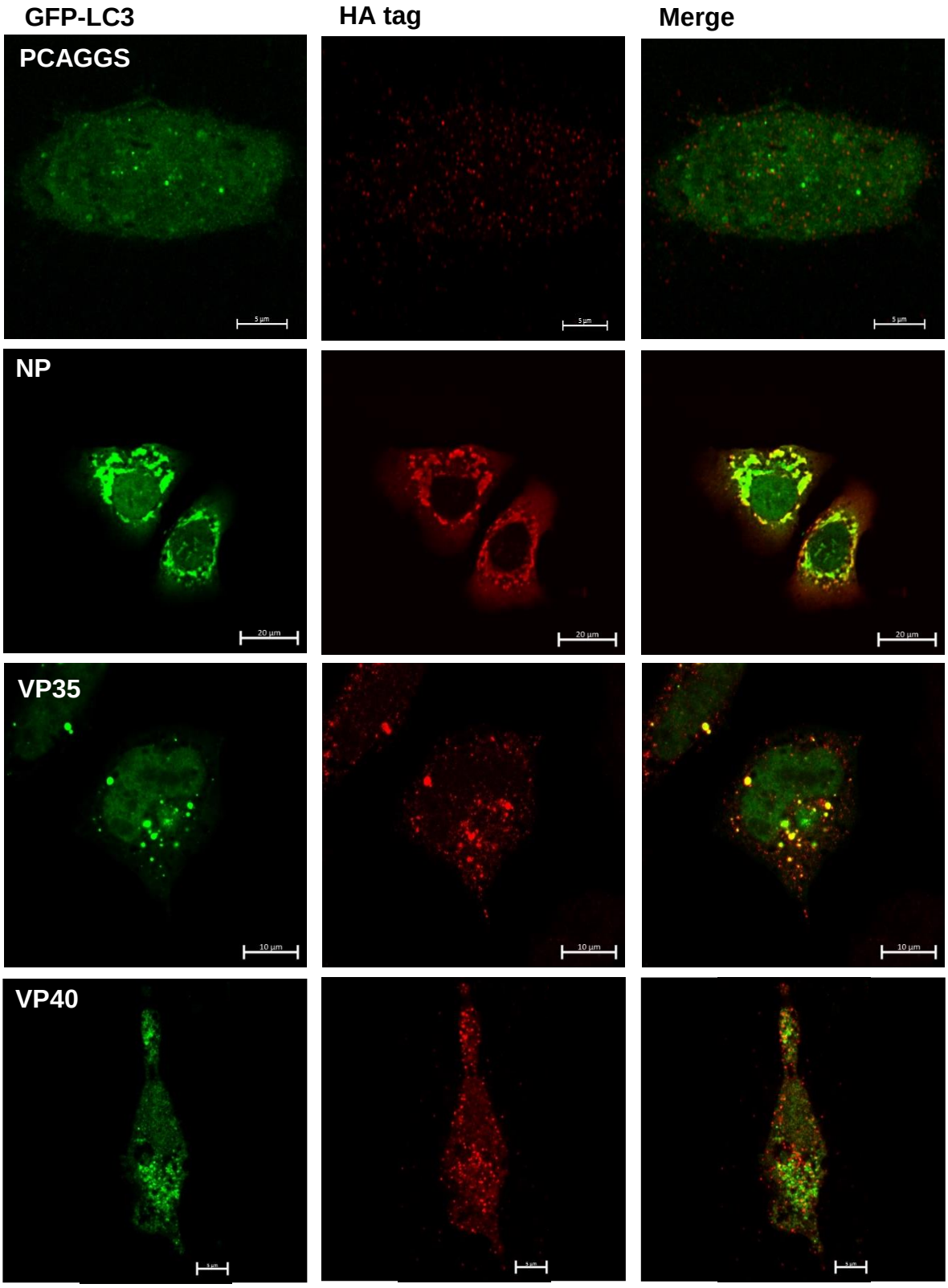

Figure 10: EBOV proteins co-localise with LC3 puncta

HeLa cells transfected with GFP-LC3 and individual EBOV protein expression plasmids.24 hours after transfection, cells were stained for HA (red) and then viewed using fluorescence confocal microscopy.

3.5 Lamp1 and LC3 co-localisation

Co-localisation of Lamp1 with the LC3 puncta can be used as an indicator to assess autophagy maturation. EBOV protein expression plamids for zNP, zVP35 and zVP40 previously seen to activate autophagy were transfected into HeLa cells along with eGFP-LC3 and Lamp1-mCherry. 48 hours later, the cells were then fixed, and stained for the HA expression tag before being imaged via fluorescence confocal microscopy. Transfection with PCAGGs was used to determine basal levels of LAMP-1 within the cell, and normal co-localisation of LAMP-1 with LC3. LAMP-1 is normally evenly distributed throughout the cell but will co-localise with LC3 in maturing autophagosomes (Figure 11). When transfected with zNP, large LC3 puncta formation occurs, and LAMP-1 is also seen to co-localise with the LC3 puncta. zNP itself can also be seen to form puncta which co-localise with both LC3 and LAMP-1 (Figure 11). The same can be seen with zVP35; LAMP-1 puncta formation occurs, and these puncta co-localise with LC3 puncta along with the zVP35 protein (Figure 11). When transfected with zVP40, Lamp1 puncta can be seen to form alongside LC3 puncta, which co-localise with the Lamp1 puncta. However, no clear zVP40 puncta can be seen (Figure 11).

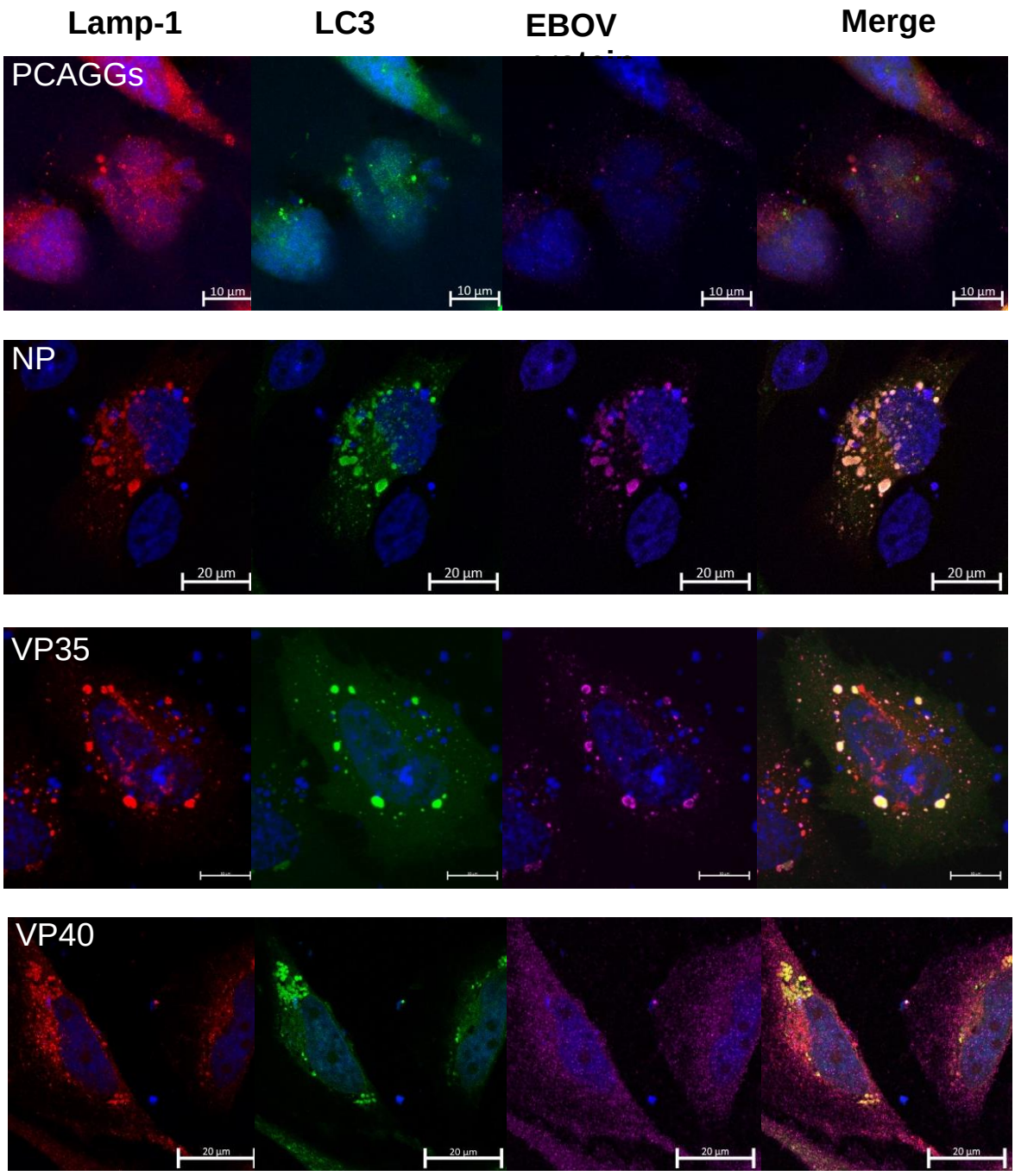

Figure 11: EBOV proteins induce autophagosome maturation

HeLa cells were co-transfected with eGFP-LC3, EBOV protein expression plasmids and mCherry-Lamp1. 48 hours post transfection, cells were fixed, and stained, before being mounted. EBOV proteins were stained pink via a HA expression tag and nuclei were stained blue with Hoechst33342. Images were viewed using fluorescence confocal microscopy. Lamp1 and LC3 puncta are seen to co-localise.

3.6 EBOV proteins increase p62 levels

Another way to determine whether maturation of the autophagy pathway is occurring is to look at the level of p62. p62 is taken into autophagosomes through selective binding to LC3 and is then degraded through autophagosomal maturation. Due to this, levels of p62 correlate inversely to autophagic maturation. HeLa cells were transfected with two positive controls; EBSS to induce autophagy via starvation, and chloroquine to inhibit autophagosomal maturation, as well as a negative control and the three EBOV protein expression plasmids seen to activate autophagy; zNP, zVP35 and zVP40. 48 hours later, cells were lysed and run on a Western Blot which was stained for p62 and imaged. Levels of p62 were quantified using the data analysis software ImageJ. When autophagy is induced via starvation, levels of p62 are decreased, while when autophagy maturation is inhibited, levels of p62 increase (Figure 12). The negative empty vector control of pCAGGs shows a p62 level in between the two positive controls, as would be expected (Figure 12). All EBOV proteins show increased levels of p62 compared to pCAGGS (Figure 12). zVP35 shows a p62 level very close to the level of the positive control of chloroquine (Figure 12).

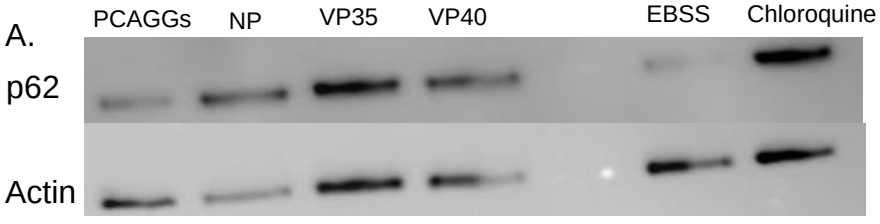

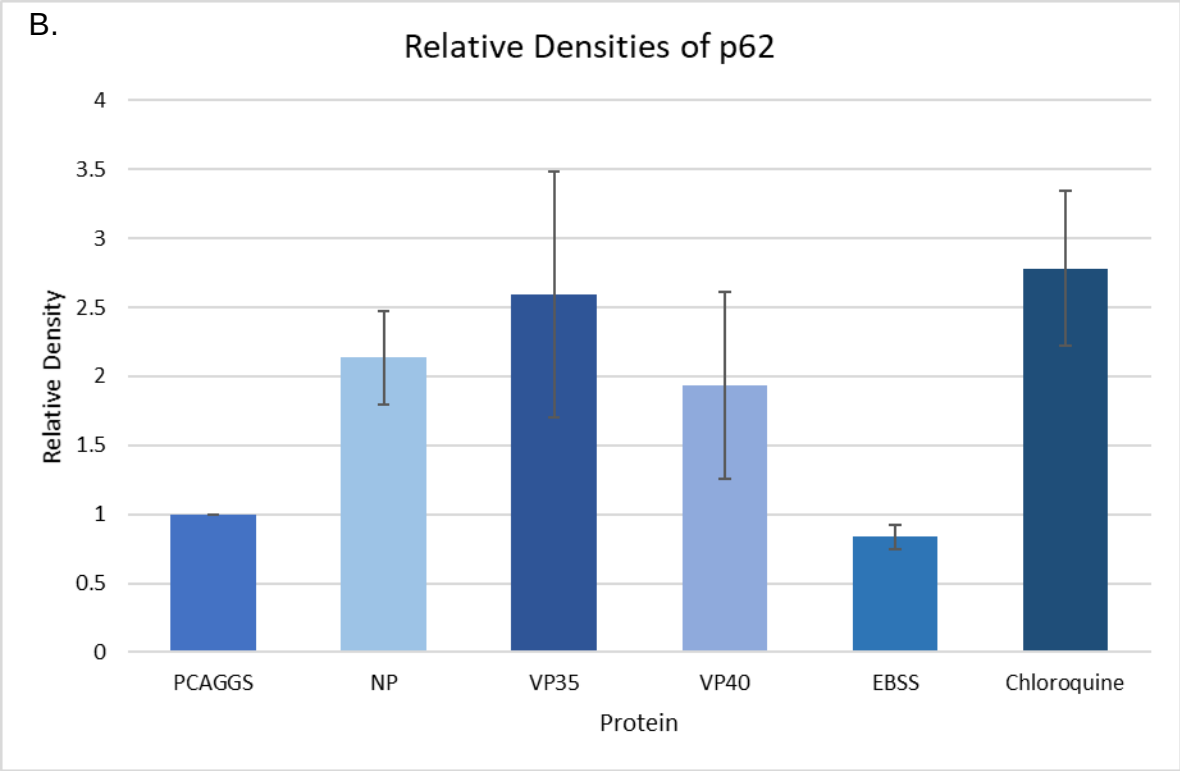

Figure 12: Specific EBOV proteins increase the level of p62 in HeLa cells

HeLa cells were transfected with negative control, or EBOV protein expressing plasmids. 44 hours later, EBSS or Chloroquine controls were added. 4 hours later, cells were lysed and run on a Western Blot

(A) Western Blot showing levels of p62 and actin in HeLa cells 24 hours post transfection.

(B) Relative density of p62 levels from 3 Western Blots. Analysed via ImageJ, with standard deviations shown.

To determine whether this increase in p62 was due to the EBOV proteins preventing the maturation of the autophagosomes, or whether they were causing an overexpression of p62, the levels of p62 in the presence or absence of chloroquine were compared. The levels of p62 increased when chloroquine was added to the negative control of PCAGGS, as would be expected (Figure 13). Levels of p62 for zNP, zVP35 and zVP40 transfected cells all stayed relatively similar in the absence and presence of chloroquine.

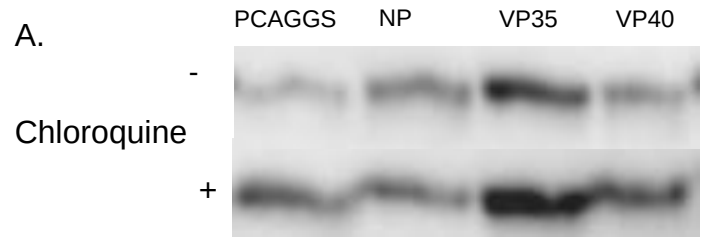

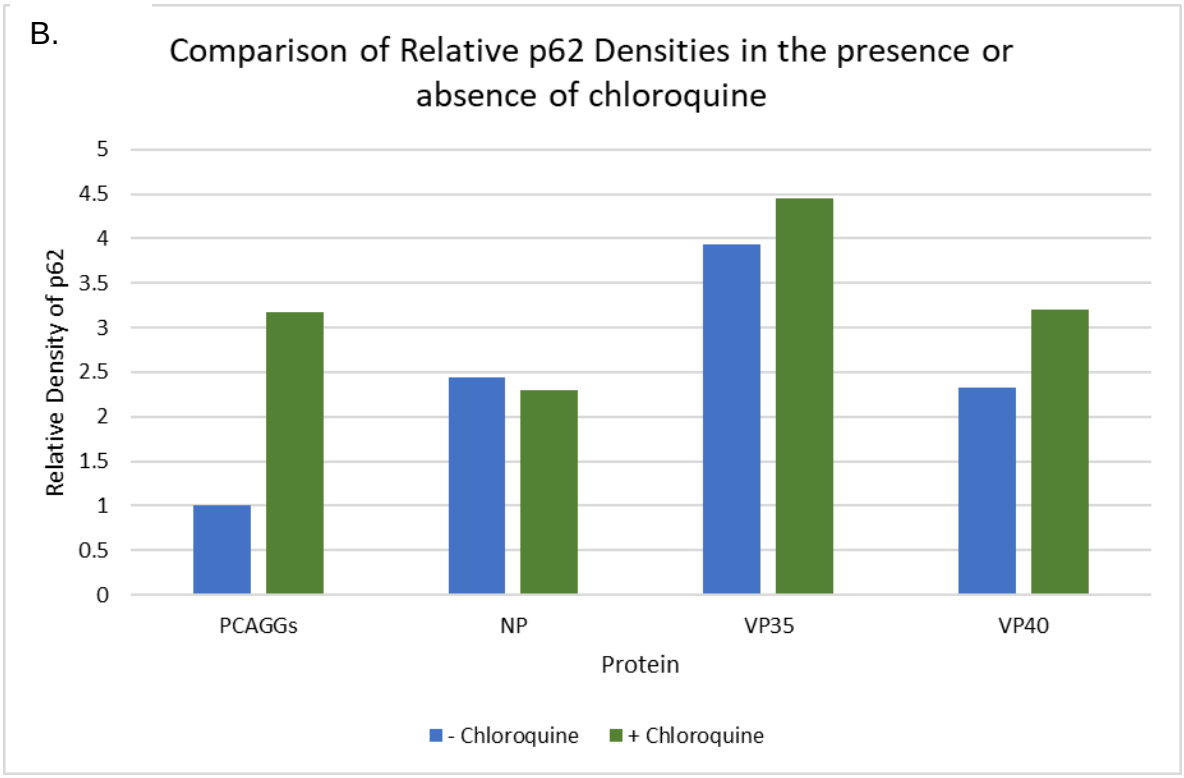

Figure 13: Levels of p62 remain similar for EBOV proteins in the absence and presence of chloroquine

HeLa cells were transfected with negative control, or EBOV protein expressing plasmids. 44 hours later, chloroquine was added to certain samples. 4 hours later, cells were lysed and run on a Western Blot

(A) Western Blot showing levels of p62 in HeLa cells in the absence or presence of chloroquine.

(B) Relative density of p62 levels in HeLa cells in the absence or presence of chloroquine. Analysed via ImageJ.

3.7 Decrease in viral replication of EBOV in HeLa-Hex cells compared to HeLa cells

To determine whether autophagy is playing a role in the replication of EBOV, a trVLP system was used [Watt,A., 2014]. A trVLP system uses a minigenome construct that encodes a luciferase gene and 3 EBOV proteins.

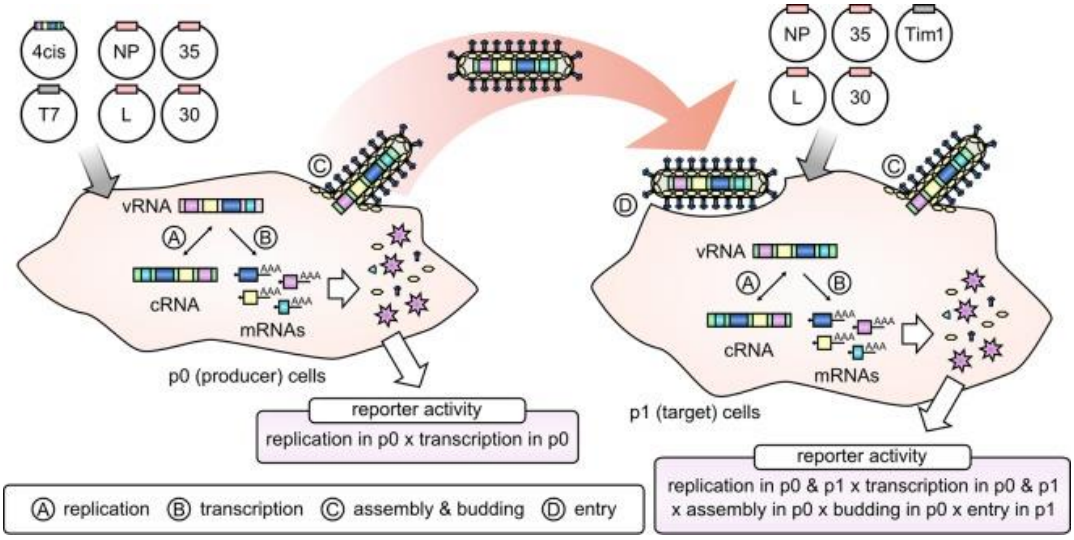

Figure 14: A schematic diagram showing the trVLP system

A schematic diagram showing the trVLP system that involves the transfection of the minigenome and four other EBOV proteins into cells where replication, transcription, and budding can occur, and the passage of these VLPs onto new cells where entry can occur [Watt,A., 2014].

This minigenome construct was transfected into HeLa or autophagy-incompetent HeLa-Hex cells along with the other 4 EBOV proteins, enabling the production of VLPs and the assessment of viral replication via luminescence. 72 hours later, the cells were lysed, and the luciferase reporter activity was determined (Table 4). To determine the background luciferase reporter activity, a negative control of untransfected cell lysate was used. Results from the HeLa and

HeLa -Hex cells were then equalised according to this control (Figure 15). Luciferase reporter activity was higher in the cell lysate from HeLa cells, when compared to the luciferase reporter activity from the HeLa- Hex cell lysates, suggesting that autophagy enhances EBOV replication (Figure 15). A student t-test was run to determine the statistical difference between the luciferase reporter activity of the HeLa and HeLa-Hex cells. The p value was less than 0.001 with a confidence interval of 95%. This difference is considered to be extremely statistically significant.

Cell Type	Sample 1	Sample 2	Sample 3	Mean
$HeLa_1$	6435	5988	6045	6156
$HeLa_2$	6695	6548	6448	6564
$HeLa_3$	7078	6963	7592	7211
Hex_1	3366	3517	3658	3514
Hex_2	3288	3471	3210	3323
Hex_3	3819	3391	3776	3662
Control	658	661	609	643

Table 4: Luciferase Reporter Activity in HeLa, HeLa -Hex and Control in p0 cells

HeLa and HeLa-Hex cells were transfected with a trVLP system containing a luciferase gene. 72 hours later, the cells were lysed. Luciferase reporter activity was measured, and the mean activity determined.

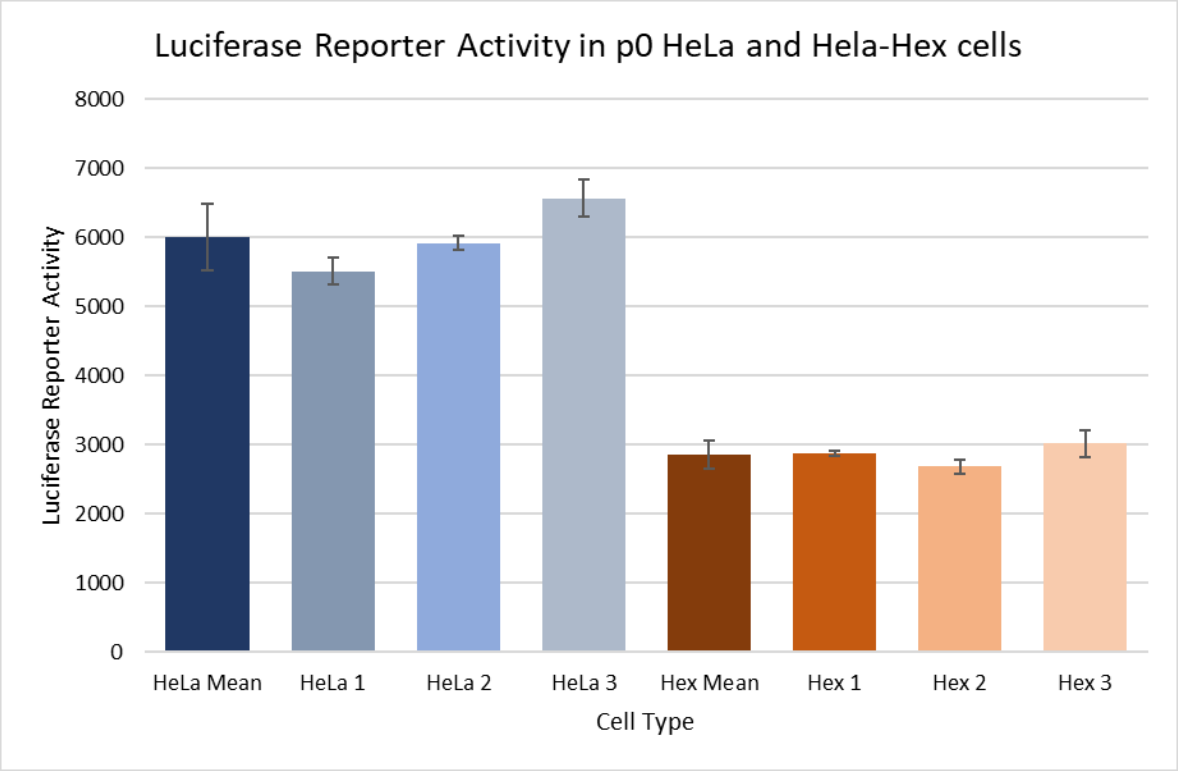

Figure 15: Luciferase Reporter Activity in p0 HeLa and HeLa - Hex cells

HeLa and HeLa-Hex cells were transfected with an EBOV trVLP system containing a luciferase gene. 72 hours later, cells were lysed. Luciferase reporter activity of cell lysates were measured and equalised to the control. Standard deviation for each measurement is shown.

3.8 Increase in budding of EBOV in HeLa-Hex cells compared to HeLa cells

To determine whether autophagy is playing a role in the budding of EBOV, the trVLP system was used. The trVLP system was transfected into HeLa or HeLa-Hex p0 cells. 72 hours later the clarified supernatants were added to p1 HeLa cells. A further 72 hours later, the cells were lysed, and the p1 luciferase reporter activity was determined, providing an indication of differences in the amount of VLPs produced by the HeLa vs HeLa-Hex p0 cells (Table 5). To determine the background luciferase reporter activity, a negative control of untransfected cell lysate was used. Results from the HeLa and HeLa-Hex VLPs were then equalised according to this control (Figure 16). Luciferase reporter activity is higher following infection with VLPs produced from HeLa p0 cells compared to HeLa-Hex p0 cells (Figure 16).

Cell Type	Sample 1	Sample 2	Sample 3	Mean
$HeLa_1$	2784	2603	2902	2763
$HeLa_2$	2128	2061	2256	2148
$HeLa_3$	2216	2096	2498	2270
Hex_1	1634	1641	1885	1720
Hex_2	1990	1844	1874	1903
Hex_3	1781	1727	1771	1760
Control	637	717	643	666

Table 5: Luciferase Reporter Activity in control and p1 HeLa cells, following infection of trVLPs produced from HeLa, HeLa-Hex and Control in p0 cells

HeLa and HeLa-Hex p0 cells were transfected with a trVLP system containing a luciferase gene. 72 hours later, the supernatant was added to p1 HeLa cells. A further 72 hours later the cells were lysed. Luciferase reporter activity was measured.

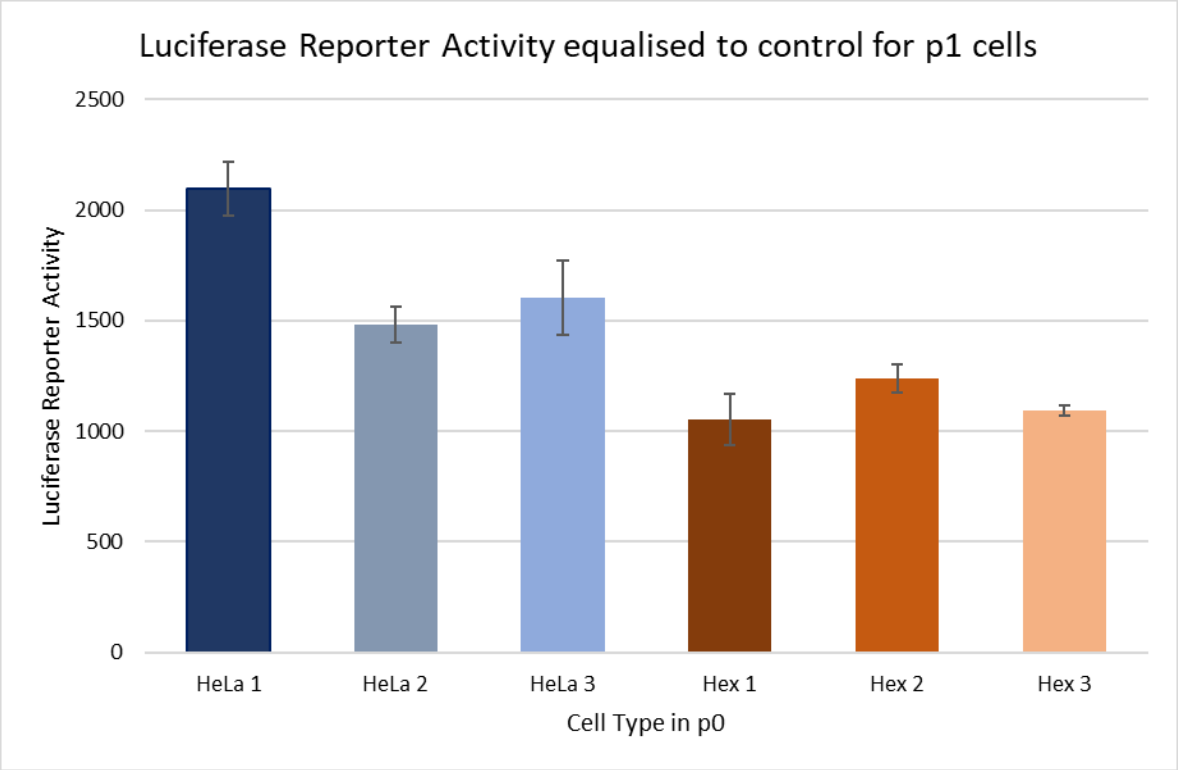

Figure 16: Luciferase Reporter Activity in HeLa p1 cells following infection with supernatant from HeLa and HeLa-Hex p0 cells

HeLa and HeLa-Hex p0 cells were transfected with an EBOV trVLP system containing a luciferase gene. 72 hours later, supernatant was added to HeLa p1 cells. Luciferase reporter activity of cell lysates of p1 cells were measured and equalised to the control. Standard deviation for each measurement is shown.

Luciferase reporter activity in p0 cells measures viral transcription and replication, whereas reporter activity in p1 cells measures VLP entry, viral transcription and replication as well as transcription, replication and budding from p0 cells. All p1 cells were HeLa cells and so should have equal entry, replication and transcription. To distinguish the impact autophagy has on budding as compared to transcription and replication, the p1 results were compared to the p0 results as the p0 results depend on only replication and transcription. The luciferase reporter activity for all cell types dropped in p1 cells compared to p0 cells

(Figure 17). A student t-test was run to determine the statistical significance of the difference between the p0 and p1 results of HeLa cells and the difference between the p0 and p1 results of HeLa-Hex cells. The p value was 0.9875 with a confidence interval of 95%. These results are considered to be not statistically significant. The percentage decrease between p0 and p1 cells was also determined (Figure 18). HeLa cells have a greater decrease between p0 and p1 cells compared to HeLa-Hex cells, suggesting that autophagy may inhibit VLP budding (Figure 18).

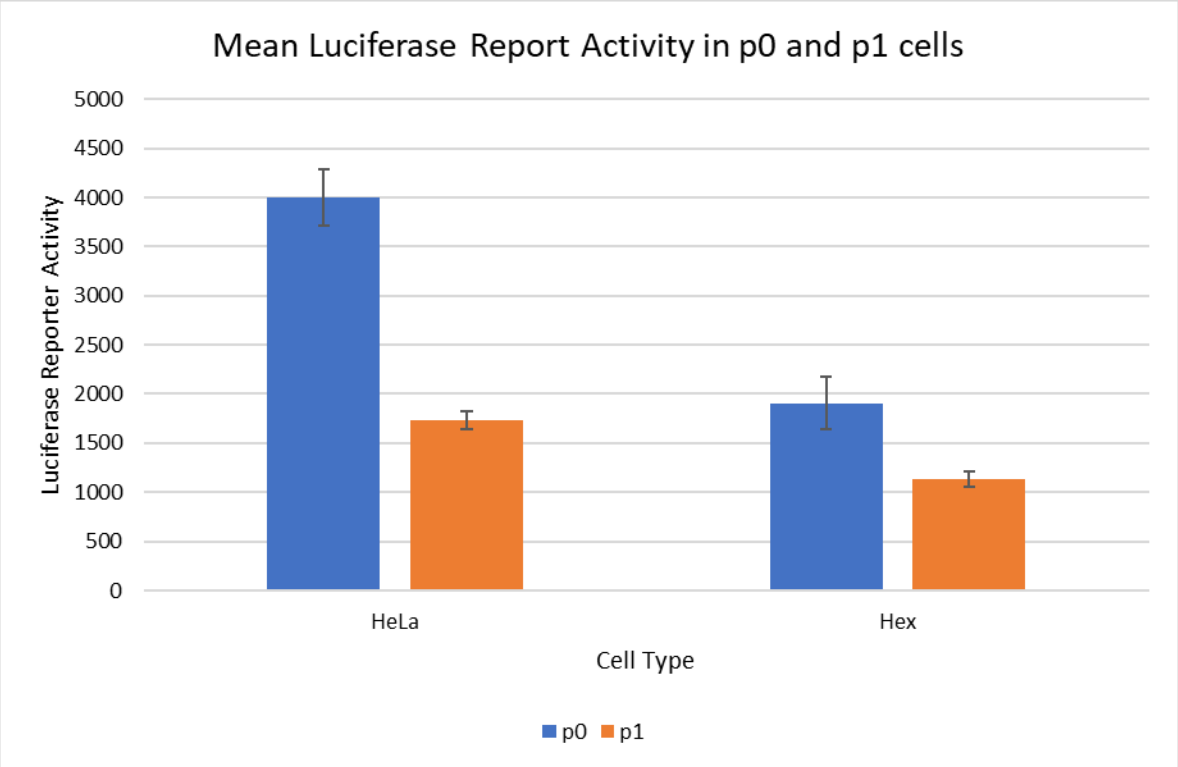

Figure 17: Comparison of luciferase reporter activity in p0 and p1 cells

The luciferase reporter activity of HeLa and HeLa-Hex p0 cells and the luciferase reporter activity of HeLa and HeLa-Hex supernatant infected HeLa p1 cells were compared. Standard deviation for each measurement is shown.

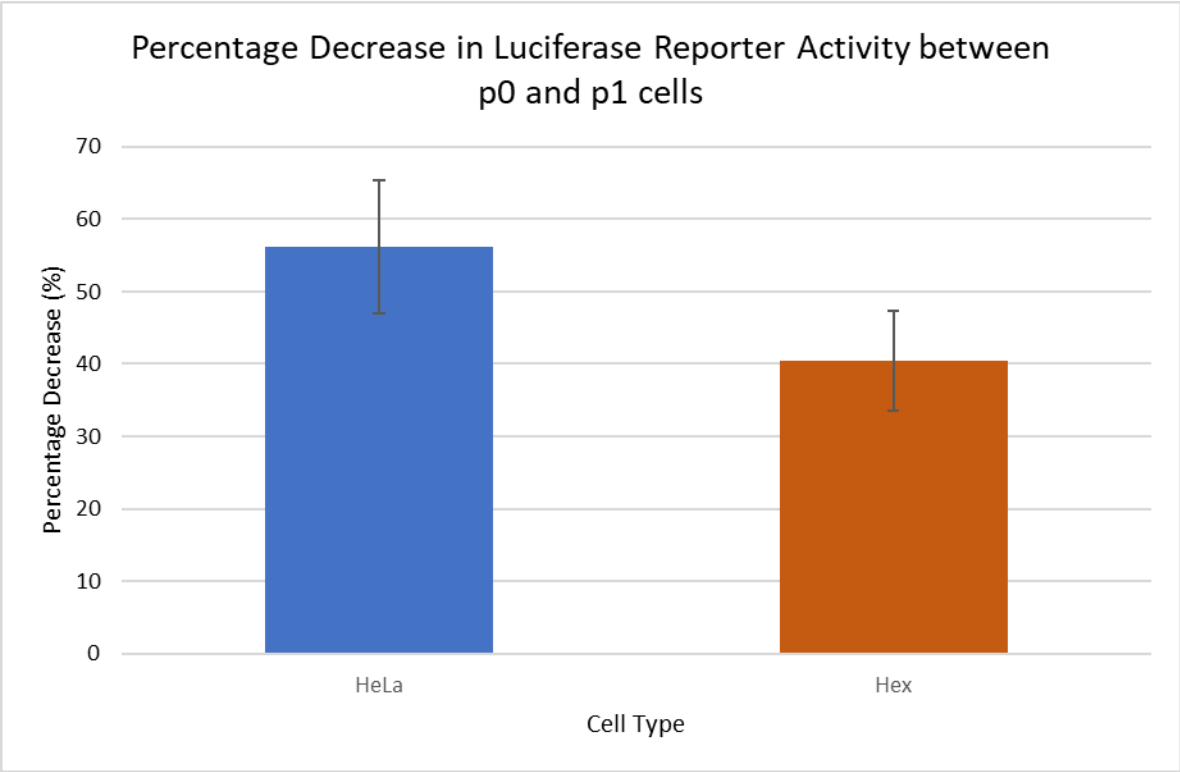

Figure 18: Percentage Decrease in Luciferase reporter activity between p0 and p1 cells

The percentage decrease between the luciferase reporter activity of HeLa and HeLa-Hex p0 cells and the luciferase reporter activity of HeLa and HeLa-Hex supernatant infected HeLa p1 cells was calculated.

4 Discussion

4.1 Introduction

This project aimed to determine if EBOV proteins are able to activate autophagy, what effect they have on the maturation of the autophagy pathway, and the overall effect the autophagy pathway has on the replication of EBOV. Through bioinformatical methods, it was determined that EBOV proteins NP, VP35, VP40 and L may activate the autophagy pathway. This was then confirmed via experimental methods; by looking for the presence of LC3 puncta. These experiments showed experimentally that NP, VP35 and VP40 can induce autophagy. Their effect on the maturation of the autophagy pathway was then determined. Lamp1 experiments showed co-localisation of Lamp1, LC3 and EBOV proteins, while p62 experiments showed increased p62 levels with EBOV proteins, suggesting complete maturation of the autophagy pathway does not occur when EBOV proteins are present. A trVLP system was then used to determine the overall effect of autophagy on EBOV replication and budding. EBOV replication was roughly halved when autophagy was inhibited, but budding seemed to increase when autophagy was inhibited, suggesting that autophagy may play a significant role in both viral replication and budding.

4.2 Determination of potential LIR domains

4.2.1 Determination of proteins that may be able to activate autophagy

Many viruses interact with the host autophagy pathway during viral infection. There is currently no published scientific literature into the activation of autophagy via EBOV proteins, therefore determining if EBOV can activate and if so which

proteins may be able to activate autophagy was a main priority. Determination of potential LIR domains present within the amino acid sequence of the seven main EBOV proteins allowed determination of the proteins that may be able to activate autophagy (Table 1). All the potential LIR domains present within the seven main EBOV protein amino acid sequences where determined using a viral LIR database [Jacomin,A-C., 2017] (Supplementary 7.1).

All the predicated LIR domains generated via the database are not likely to be functional. To determine which ones were most likely to be functional, the PSSM score generated via the database was used. The PSSM score is a position specific scoring matrix generated by the database and is based on a log-odds score of a residue being present at a specific position [Kalvari,I., 2014]. The higher the PSSM score, the more likely it is that the domain is functional. PSSM scores of previously experimentally determined LIR domains, and the specificity and sensitivity scores of different PSSM's were used to determine the lower PSSM score limit for this study. A PSSM score limit of 11 was set.

Four EBOV proteins contained LIR domains that satisfied the criteria set out; zVP35, zVP40, zL and zNP as seen in Table 1. This suggests that these four proteins may be able to activate autophagy. Only one experimentally determined viral LIR domain exists, an LIR domain in the tail end of the M2 protein of the Influenza A virus [Beale,R.,2014]. This domain allows the M2 protein to directly bind to LC3, and cause LC3 to translocate to the plasma membrane. When LC3 binding is inhibited via mutations, there is reduced virion stability and interference with filamentous budding [Beale,R.,2014]. The LIR domains identified within the EBOV proteins may also act in the same way, subverting the autophagy pathway to aid in

viral replication, or could interact with the autophagy pathway in an alternative way.

4.2.2 Difference in potential LIR domains between EBOV and RESTV

RESTV is the only Ebolavirus species that is non-pathogenic to humans, but the reason for this difference is still to be determined. A reason for this difference could lay in different interactions with the autophagy pathway between RESTV and the other Ebolavirus species. The RESTV protein amino acid sequences of the seven main RESTV proteins were run through the LIR database [Jacomin,A-C., 2017] (Supplementary 7.2). The same criteria that was previously applied to the EBOV proteins was applied to the potential LIR domains present within the RESTV proteins. There were more potentially functional domains present within RESTV proteins compared to EBOV proteins as seen in Table 2. There were five RESTV proteins that contained potentially functional domains, with four of these being the same proteins seen in EBOV, with rGP being the only new protein to show potentially functional LIR domains. The increase in domains suggests that RESTV proteins may be able to activate the autophagy pathway better than EBOV proteins.

4.2.3 Crossover of LIR domains with SDP's

Specificity Determining Positions are amino acids that stay the same within sub-species but differ between species. 189 SDP's have been determined between RESTV and the pathogenic strains of Ebolavirus [Pappaardo,M., 2016]. These SDPs could account for the difference seen in the amount and likely functionality of the LIR domains between EBOV and RESTV. To test this hypothesis, the potentially

functional LIR domains present within RESTV were cross referenced with the known SDPs present within RESTV. Five of the potentially functional LIR domains present within RESTV crossed over with SDPs as seen in Table 3. This crossover resulted in the presence of three potentially functional LIR domains in RESTV proteins which aren't present in EBOV, while two potentially functional LIR domains had higher PSSM scores in RESTV compared to EBOV. The crossover of the SDPs with the LIRs appears to increase the presence of LIRs and the ability to bind to LC3, thus making it likely that they are increasing the interaction of the proteins with the host autophagy pathway. This could suggest that autophagy is acting in anti-viral way during Ebolavirus infection, and this is what leads to difference seen in pathogenicity between EBOV and RESTV. However, there is a lot of conservation of LIRs domains between EBOV and RESTV. This conservation of LIRs domains could suggest that autophagy is essential for efficient viral replication, and so cannot be mutated between species without losing viral replication. The difference seen in LIRs domains would then suggest that increasing autophagy could limit some part of the Ebolavirus life cycle, limiting viral replication in some way in RESTV compared to EBOV, leading to the difference in pathogenicity.

4.3 Autophagy induction by specific EBOV proteins

After determining which proteins may be able to activate autophagy via bioinformatics, an experimental method was used to test which ones could activate autophagy within the laboratory setting. This was done by looking for the presence of autophagosomes via immunofluorescence microscopy. GFP-LC3 is a fusion protein where GFP is present at the amino terminus of LC3. During autophagy LC3

becomes conjugated with PE to form LC3-II, which associates with both the inner and outer membranes of autophagosomes [Mizushima,N., 2010]. Using the fusion protein GFP-LC3, the presence of LC3 can be viewed via immunofluorescence, with it being either diffuse throughout the cytoplasm, or as punctate structures that represent autophagosomes [Mizushima,N., 2010] .

Previous work carried out in MEF cells had showed that zNP and zVP35 were able to cause autophagy induction (Supplementary 7.3). These results were confirmed with zVP35 and zNP still showing autophagy induction as seen in Figure 8. Of the other EBOV proteins tested, zVP30 and zVP40 also showed autophagy induction as seen in Figure 8.

Autophagy is highly cellular specific [Sharifi,M,N., 2015], and EBOV proteins have different interactions in mouse cell lines compared to human cell lines [Martinez,O., 2013]. Due to this, autophagy induction was also tested in the human cell line HeLa. zVP35, zVP40 and zNP again all showed autophagy induction, as seen in Figure 9. In comparison to the induction of autophagy in the MEF cell line, all three proteins were able to induce autophagy to a greater degree in the HeLa cell line, with more puncta being seen throughout the cells. Within the HeLa cell line, zNP can be seen to cause the formation of large aggregates which are indicative of significant activation of the autophagy pathway. However, zVP30 showed no formation of LC3 puncta, suggesting that within a human cell line zVP30 is not able to activate autophagy.

Previous work showed that Marburg NP, a protein very similar to EBOV NP, was able to cause the formation of LC3 positive punctate structures, when large Marburg NP inclusions were formed [Dolnik, O.,2015]. Marburg uses inclusion bodies

for RNA synthesis in the same way as EBOV. This paper suggested that Marburg may regulate the autophagy pathway during infection either usurping it for viral replication or acting as a target for the autophagosomal pathway [Dolnik,O., 2015]. These results suggest that these EBOV proteins could be activating autophagy via similar methods as Marburg as similar results have been seen, and the proteins themselves have similar structures and similar roles within viral infection.

zNP and zVP35 both play an important role in the replication of EBOV, with both being involved in the formation of the replication complex and inclusion bodies synthesis [Mahanty, 2004] [Hoenen, T.,2012]. Inclusion bodies are the sites of viral RNA synthesis within Ebolavirus, as well as being the site where nucleocapsids of differing maturation are found [Dolnik,O., 2015]. The induction of autophagy via these EBOV proteins suggests that autophagy may play a role in the replication of EBOV, such as aiding in the formation of the inclusion bodies, or bringing cellular components to the inclusion bodies. However, the other protein that induced autophagy, zVP40, does not play a role in replication, but is required for transport of the inclusion bodies to the plasma membrane, as well as being essential in viral egress [Noda, T., 2006] [Han, Z., 2017]. This suggests that autophagy could be also play a role in viral transport throughout the cell, and then viral egress.

4.4 Co-localisation of LC3 puncta with EBOV proteins

To determine whether the EBOV proteins were interacting with the autophagosomes, or were just inducing the autophagy pathway, co-localisation of LC3 puncta and EBOV proteins was determined. As seen in Figure 10, the EBOV proteins that had been seen to activate autophagy; zNP, zVP35 and zVP40 all co-localised with the LC3 puncta's, although to varying degrees.

Co-localisation of the EBOV protein with LC3 puncta suggests that the proteins themselves are interacting with the autophagosome in some way. Interaction with autophagosomes could suggest that EBOV proteins are being selectively targeted via the autophagy pathway for degradation via the autolysosome. During HIV-1 infection, the HIV-1 protein Tat, which is essential for viral transcription and virion production, is selectively degraded via the autophagy pathway [Sagnier,S., 2015]. This degradation could be happening during EBOV infection. However, it could also suggest that the EBOV proteins are subverting the autophagy pathway, and are using the autophagosomes to aid in viral infection, such as during Polio viral infection, during which it appears that the autophagy pathway acts in a pro-viral way, facilitating viral replication within the cell [Jackson,W.,T., 2005]. .

4.5 Co-localisation of LC3 puncta with Lamp1

Increased levels of LC3 puncta can be associated with either an increase in autophagosome synthesis or reduced autophagosomal turnover [Barth,S., 2010]. Reduced autophagosomal turnover could occur due to a variety of reasons such as reduced fusion with lysosomes or endosomes, or delayed trafficking to the lysosomes [Barth,S., 2010].

To determine whether the EBOV proteins were reducing the autophagosomal turnover, and therefore the maturation of the autophagy pathway, the co-localisation of Lamp1 with LC3 puncta was investigated. Lamp1 is a lysosomal protein that is trafficked to autophagosomes during maturation [Jackson,W.,T., 2005], and so can be used to determine if there is reduced autophagosomal turnover. As can be seen from Figure 11, Lamp1 puncta that co-localise with LC3 puncta can be

seen for zNP, zVP35 and zVP40. This suggests that fusion of the autophagosomes and lysosomes is occurring.

Previously, it has been seen that Lamp1 is recruited into Marburg NP inclusions, and that co-expression of NP and VP40 causes co-localisation of Lamp1 with VP40 in VP40 clusters, and NP inclusions containing VP40 [Dolnik, O.,2015]. However, Lamp1 is an endolysosomal marker, and is seen in other pathways as well as autophagy. The co-localisation of LC3 with Lamp1 within these clusters and inclusions was not visualised during the study which could mean that the interaction seen with Marburg proteins was not due to maturation of autophagosomes.

However, the co-localisation of Lamp1 and LC3 has been seen in viruses that do interact with the autophagy pathway during viral infection. During poliovirus infection, LC3 containing double-membrane vesicles have been identified. Within these vesicles, LC3 and Lamp1 are seen to co-localise [Jackson,W.,T., 2005]. During poliovirus infection, it appears that the autophagy pathway and the production of these vesicles act in a pro-viral way, facilitating viral replication within the cell [Jackson,W.,T., 2005]. Therefore, the co-localisation of Lamp1 with LC3 and the EBOV proteins could suggest that the virus is subverting the pathway to aid in viral replication, as two of the proteins that activate the pathway are involved in the formation of the replication complex for EBOV.

Alternatively, the co-localisation of Lamp1 and LC3 could suggest that the autophagy pathway is reaching maturation and is causing the degradation of EBOV proteins that have been taken up into the autophagosomes. This would

suggest that the pathway is acting in an anti-viral way, removing vital viral proteins from the cell, hindering the replication of the virus.

4.6 EBOV proteins prevent autophagic flux

To determine if the degradation of the proteins present within the autophagolysosmes occurs, levels of p62 were investigated. p62 interacts with LC3 and is then degraded by autophagy [Barth,S., 2010]. Due to this, levels of p62 can be used to determine autophagic flux, with p62 levels correlating inversely with autophagy. As can be seen in Figure 12, all three EBOV proteins, zNP, zVP35 and zVP40 cause an increase in p62 levels compared to the negative control. This could be due to the proteins preventing autophagic flux and the degradation of autophagolysosmes, or it could be due to the proteins causing an overexpression of p62. To determine which scenario is occurring, the autophagic flux inhibitor chloroquine was used. If the EBOV proteins were causing an overexpression of p62, when chloroquine is added, levels of p62 will increase as degradation of the overexpressed p62 will be prevented. As can be seen from Figure 13, levels of p62 in the EBOV protein samples are relatively similar in the absence and presence of chloroquine, suggesting that the proteins are not causing an overexpression of p62, but are preventing autophagic flux.

Other viruses are known to inhibit autophagic flux to aid in viral replication. During the reactivation of Epstein-Barr virus from latency, the autophagy pathway is activated but autophagic flux is blocked [Granato,M., 2014]. This block of autophagic flux can be attributed to the down regulation of the autophagosomal maturation protein, Rab7 [Wang,M., 2015]. Blocking autophagic flux allows the Epstein-Barr virus to use the autophagic vesicles for intracellular transportation and

viral production [Granato,M., 2014]. Preventing autophagic flux may also allow Epstein-Barr virus to avoid degradation by the autolysosome [Wang,M., 2015]. The induction and then subversion of the autophagy pathway seen by EBOV could indicate that the autophagy pathway is playing an important role in EBOV replication.

4.7 Decrease in replication of EBOV in HeLa-Hex cells compared to HeLa cells

To determine if the autophagy pathway plays a role in the replication of EBOV, a trVLP system, as seen in Figure 19, was used in HeLa and HeLa-Hex cells.

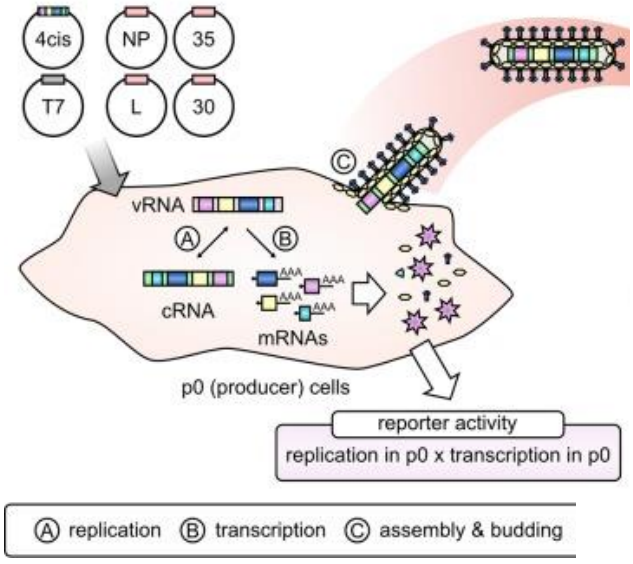

Figure 19: Schematic diagram to show trVLP system in p0 cells

A schematic diagram showing the transfection of plasmids and minigenome into the cell. The minigenome is then replicated and transcribed before assembly and budding occurs [Watt,A., 2014].

The replication and transcription of EBOV can then be tested for by looking at the reporter activity of luciferase. Hex cells are HeLa cells that have all eight variants of the ATG8 (LC3) protein knocked out. Due to this, HeLa-Hex cells can be used to compare replication rates of EBOV between autophagy deficient and normal cells. As can be seen from Figure 15, the luciferase reporter activity is

greatly reduced in p0 HeLa-Hex cells compared to HeLa cells. This suggests that when the autophagy pathway is removed from cells, EBOV is unable to replicate as effectively.

NP and VP35 are both vital proteins required in the replication of EBOV. Along with VP30 and L, they form the replication complex required to generate mRNA transcripts and full-length positive sense RNA antigenomes, which act as templates for genome synthesis [Mahanty, 2004]. As well as forming the actual replication complex, NP and VP35 are both involved in the formation of inclusion bodies which act as the site of viral replication [Hoenen,T.,2012]. The activation of autophagy by these two proteins, and the reduction of EBOV replication seen in HeLa-Hex cells suggests that the interaction of these two proteins with the autophagy pathway could be linked to their roles in the replication cycle of EBOV. These proteins could be using the autophagic vesicles for viral production as seen in Epstein-Barr viral infection [Granato,M., 2014].

4.8 Increase in budding of EBOV in HeLa-Hex cells compared to HeLa cells

To determine the effect the autophagy pathway has on the budding of EBOV, the trVLP system was used. After replication and transcription has taken place in the p0 cells, VLP's bud from the cells and are released into the supernatant. This supernatant can then be clarified and placed onto new cells, p1, where entry and replication of the VLP's in the new cells can take place, as seen in Figure 20.

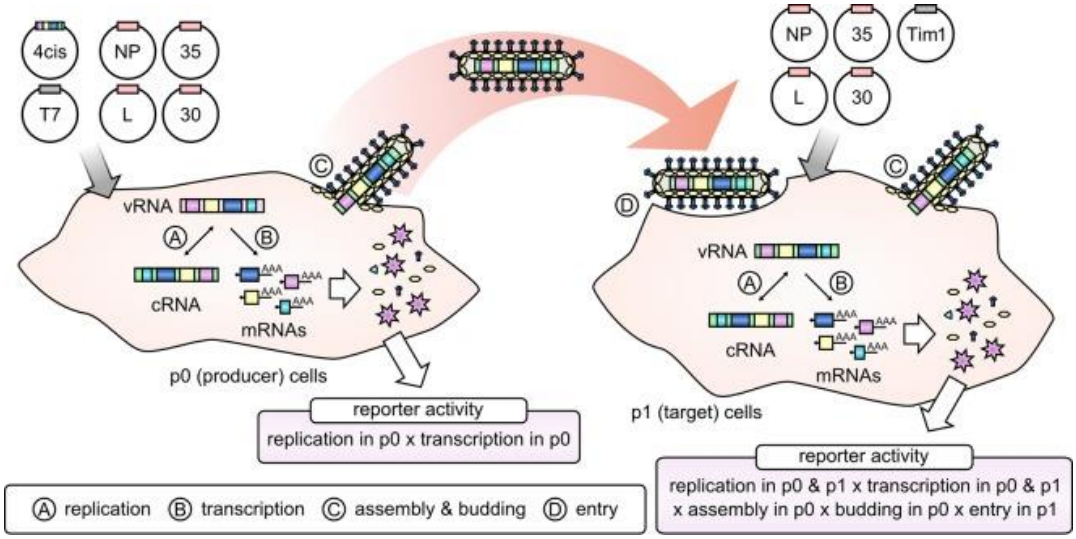

Figure 20: A schematic diagram to show trVLP system in p0 and p1 cells

A schematic diagram showing the transfection of plasmids and minigenome into p0 cells. The minigenome is then replicated and transcribed before assembly and budding occurs. The supernatant is then passaged onto new p1 cells [Watt,A., 2014]

To determine the effect autophagy has on budding, the trVLP system can be transfected into HeLa and HeLa-Hex p0 cells, then passaged onto HeLa p1 cells, meaning autophagy only plays a role in the replication, transcription and budding that occurs in p0 cells. As can be seen from Figure 16, luciferase reporter activity is still slightly higher in the p1 cells with HeLa p0 supernatant, compared to the p1 cells with HeLa-Hex supernatant. However as seen from Figure 18, the percentage decrease from the luciferase reporter activity from p0 to p1 HeLa cells is greater than the percentage decrease seen in HeLa-Hex p0 cells, although this difference is not statistically significant. However, it could still suggest that there was less

budding from the HeLa cells, causing a decrease in the luciferase reporter activity seen in the p1 cells. This suggests that autophagy is preventing the budding of EBOV in some way.

VP40, one of the proteins seen to cause induction of autophagy is essential for the budding of EBOV. VP40 is required for the transport of the nucleocapsids to the plasma membrane [Noda,T., 2006]. VP40 then recruits vital proteins for viral egress, allowing the release of the newly synthesised viral particles [Han,Z., 2017]. The apparent increase in budding from HeLa-Hex cells compared to HeLa cells suggests that the interaction of VP40 with the autophagy pathway could be acting in an anti-viral way.

However, the results seen in Table 5 are affected by transcription, replication and budding within p0. Figure 15 clearly shows that there is a difference in the transcription and replication between HeLa and HeLa-Hex cells. It is logical to assume that increased replication would also lead to increased levels of budded virions but this budding could be affected by other scenarios, such as maximal budding limits for HeLa and HeLa-Hex cells. If the maximal budding limit for the HeLa's was reached during the experiments, but not for the HeLa-Hex cells, this could lead to inaccurate representations of the amount of budding that occurs. This would mean that the greater decrease in luciferase reporter activity seen in the HeLa's may not accurately represent the true budding ability of the HeLa's. This could affect the luciferase reporter activity seen in Table 5, and so affect the conclusions on the effect autophagy has on budding.

4.9 Conclusion

In this study it has been shown that certain EBOV proteins, zNP, zVP35 and zVP40 are able to induce the autophagy pathway and co-localise with the autophagosomes produced. These autophagosomes then appear to undergo fusion with the lysosomes, but do not undergo full maturation, with autophagic flux being prevented. The overall autophagy pathway appears to play a role in the viral replication of EBOV. Ebolavirus could induce the autophagy pathway to aid in the formation of inclusion bodies which are essential for viral replication. However, robust autophagy could then hinder viral budding, perhaps by preventing transport of key viral components to the plasma membrane.

Future experiments could aid in confirming and developing the knowledge of the interaction of EBOV with the autophagy pathway. Experiments to confirm the role of autophagy in the budding of EBOV need to be carried out, to eliminate the possibility that other factors played a role in the decrease seen in luciferase reporter activity seen in Figure 17. To determine that there is no budding limit, and that increases in budding correlates with increases in replication, a trVLP experiment which alters the levels of plasmid DNA transfected, but not the ratio of plasmids could be run. The luciferase reporter activity for p0 and p1 could then be analysed. If there is no budding limit, and budding and replication do correlate, then the luciferase reporter activity of p0 and p1 should both decrease as plasmid concentration decreases. This would then allow the exact determination of the role autophagy plays in the budding of EBOV.

To try and develop a greater understanding of the interaction of the EBOV proteins with LC3, LIR mutants based on the predicted LIR domains listed in this

study could be created. Experiments looking into the effect these mutants have on the induction of autophagy could help to understand the exact interaction occurring between EBOV proteins and LC3. RESTV LIR domains were determined during this study, but the interaction of RESTV proteins with the autophagy pathway were not studied due to time constraints. These experiments could provide a greater understanding into the different pathogenicity seen between RESTV and the other Ebolavirus species.

The results determined via this study provide a greater understanding into the interaction that EBOV proteins have with the cellular autophagy pathway during infection. Understanding the effect EBOV has on cellular processes leads to a greater understanding of how the virus is able to survive and reproduce within the host which can lead to the development of novel therapeutic targets. Studies have shown that inhibiting autophagy during viral infections can lead to a decrease in viral titre and viral replication. An autophagy inhibitor, spautin-1, was able to greatly affect the production of infectious particles of dengue virus [Mateo,R., 2013]. Spautin-1 is a highly selective early stage autophagy inhibitor, with it being able to cause the degradation of the Beclin-Vps34-Atg14 complex, as well as decreasing intracellular concentrations of phosphatidylinositol 3-phosphate, a lipid required for the initiation of autophagosome formation [Mateo,R., 2013]. An autophagy inhibitor like this could be tested against EBOV to see the effect it has on viral replication. Currently derivates of spautin-1 are being developed as therapeutic drugs to target autophagy [Kotz,J., 2011], which could eventually act as a therapeutic drug against viruses that subvert the autophagy pathway for viral replication.

5 References

1 Alemu,E.A., Lamark,T., Torgersen,K.M., Birgisdottir,A.B.. Larsen,K.B., Jain,A., Olsvik,H., Overvatn,A., Kirkin,V., and Johansen,T.(2012) Atg8 Family Proteins Act as Scaffolds for Assembly of the ULK Complex. Journal of Biological Chemistry,16,287,39275-39290

2 Barrette,R.W., Metwally,S.A., Rowland,J.M., Xu,L., Zaki,S.R., Nichol,S.T., Rollin,P.E., Towner,J.S., Shieh,W-J., Batten,B., et al (2009) Discovery of Swine as a Host for the Reston ebolavirus. Science, 325, 204-206

3 Barth,S., Glick,D., and Macleod,K.,F. (2010) Autophagy: Assays and Artifacts. Journal of Pathology, 221, 117-124

4 Bausch,D.G., Towner,J.S., Dowell,S.F., Kaducu,F., Lukwiya,M. Sanchez,A., Nichol,S.T., Ksiazek,T.G., and Rollin,P.E. (2007) Assessment of the Risk of Ebola Virus Transmission from Bodily Fluids and Fomites. Journal of Infectious Diseases, 196, Supplement 2, S142-S147

5 Beale,R., Wise,H., Stuart,A., Ravenhill,BJ., Digard,P., Randow,F. (2014) A LC3-interacting motif in the influenza A virus M2 protein is required to subvert autophagy and maintain virion stability. Cell Host Microbe, 12, 239-47

6 Boehmann,Y., Enterlein,S., Randolf,A., and Muhlberger,E. (2005) A reconstituted replication and transcription system for Ebola virus Reston and comparison with Ebola virus Zaire. Virology, 332, 406-417

7 Bray,M., and Geisbert,T,W. (2005) Ebola virus: The role of macrophages and dendritic cells in the pathogenesis of Ebola hemorrhagic fever. International Journal of Biochemistry & Cell Biology, 37,1560-1566

8 Chiramel,A.I., Brady,N.R., Bartenschlager,R. (2013) Divergent Roles of Autophagy in Virus Infection. Cells, 2, 83-104.

9 Chiramel,A.I., Dougherty,J.D., Nair,V., Robertson,S.J., Best,S.M. (2016) FAM134B, the Selective Autophagy Receptor for Endoplasmic Reticulum Turnover, Inhibits Replication of Ebola Virus Strains Makona and Mayinga. The Journal of Infectious Diseases, 214, S319-325

10 Dolnik,O., Stevermann,L., Kolesnikov,l., Becker,S. (2015) Marburg virus inclusions: A virus- induced microcompartment and interface to multivesicular

bodies and the late endosomal compartment. European Journal of Cell Biology, 94, 323-331.

11 Feldmann,H., Geisbert,T,W. (2011) Ebola Haemorrhagic Fever. Lancet, 377, 849-862

12 Fujita,N., Itoh,T., Omori,H., Fukuda,M., Noda,T., and Yoshimori,T. (2008) The Atg16L Complex Specifies the Site of LC3 Lipidation for Membrane Biogenesis in Autophagy.

13 Granato,M., Santarelli,R., Farina,A., Gonnella,R., Vittoria Lotti,L., Faggioni,A., Cirone,M. (2014) Epstein-Barr Virus Blocks the Autophagic Flux and Appropriates the Autophagic Machinery to Enhance Viral Replication. Journal of Virology, 88, 12715-12726

14 Han,Z., Sagum,C.A., Takizawa,F., Ruthel,G., Berry,C.T., Kong,J., Oriol SUnyer,J., Freedman,B.D., Bedford,M.T., Sidhu,S.S., et al (2017) Ubiquitin Ligase WWP1 Interacts with Ebola Virus VP40 to Regulate Egress. Journal of Virology, 91,

15 He,C., and Klionsky,D.J. (2009) Regulation Mechanisms and Signaling Pathways of Autophagy, Annual Review of Genetics, 43, 67-93

16 Hoenen,T., Shabman,R.S., Groseth,A., Herwig,A., Weber,M., Schudt,G., Dolnik,O., Basler,C., F., Becker,S., and Feldmann,H. (2012) Inclusion Bodies are a Site of Ebolavirus Replication. Journal of Virology, 86, p11779-11788

17 Hosokawa,N., Hara,T., Kaizuka, T., Kishi,C., Takamura,A., Miura,Y., Iemura,S-I., Natsume,T., Takehana,K., Yamada,N., et al. (2009) Nutrient-dependent mTORC1 Association with the ULK1-Atg13-FIP200 Complex Required for Autophagy. Molecular Biology of the Cell, 20, 1981-1991.

18 Huynh,K.K., Eskelinen,E-L., Scott,C.C., Malevanets,A., Saftig,P., and Grinstein,S. (2007) LAMP proteins are required for fusion of lysosmes with phagosomes. EMBO Journal, 26, 313-324

19 Ichimura,Y., and Komatsu,M. (2010) Selective degradation of p62 by autophagy. Seminars in Immunopathology, 32, 431-436

20 Jackson,W.,T., GiddingsJr,T.,H., Taylor,M.,P., Mulinyawe,S., Rabinovitch,M., Kopito,R.,R., Kiregaard,K. (2005) Subversion of Cellular Autophagosomal Machinery by RNA Viruses. PLOS Biology, 3, e156

21 Jacomin,A-C., Samavedam,S., Charles,H., and Nezis.,I.P. (2017) iLIR@viral: A web resource for LIR motif-containing proteins in viruses. Autophagy, 13,10,1782-1789

22 Jager,S., Bucci,C, Tanida,I., Ueno,T., Kominami,E., SAftig,P. and Eskelinen,E-L. (2004) Role for Rab7 in maturation of late autophagic vacuoles. Journal of Cell Science, 117, 4837-48487

23 Kalvari,I., Tsompanis,S., Mulakkal,N.C., Osgood,R., Johansen,T., Nezis,I., and Promponas,V.I.(2014) iLIR A web resource for predicition of Atg8-family interacting proteins. Autophagy,10,5,913-925

24 Kash,J.C., Muhlberger,E., Carter,V., Grosch,M., Perwitasari,O., Proll,S.C., Thomas,M.I., Weber,F., Klenk,H-D., and Katze,M.G. (2006) Global suppression of the host antiviral response by Ebola- and Marburgviruses: increased anatagonsim of the type I interferon response is associated with enhanced virulence Journal of Virology, 80, 3009-3020

25 Khaminets, A., Heinrich,T., Mari,M., Grumati,P., Huebner,A.K., Akutsu,M., Liebmann,L., Stolz,A., Nietzche,S., Koch,N., et al. (2015) Regulation of Endoplasmic Reticulum Turnover by Selective Autophagy. Nature, 522, 354-358

26 Kotz,J. (2011) Anaylsis: Target and Mechanism – Cancer. SciBX, 4

27 Kuhn,J.H., Becker,S., Ebihara,H., Geisbert,T.W., Johnson,K.M., Kawaoka,Y., Lipkin,W.I., Negredo,A.I., Netesov,S.V., Nichol,S.T., et al (2010) Proposal for a revised taxonomy of the family Filoviridae: classification, names of taxa and viruses, and virus abbreviations. Archives of Virology, 12, 2083-2103

28 Lefebvre,A., Fiet,C., Belpois-Duchamp,C., Tiv,M., Astruc,K., and Aho Glele, L.S. (2014) Case fatality rates of Ebola virus diseases: A meta-analysis of World Health Organisation data. Medecine et Maladies Infectieuses, 44, 412-41

29 Leroy,E.M., Kumulungi,B., Pourrut,X., Rouquet,P., Hassanin,A., Yaba,P., Delicat,A., Paweska,J.T., Gonzalez,J-P., and Swanpoel,R. (2005) Fruit bats as reservoirs of Ebola virus. Nature, 438, 575-576

30 Mahanty,S. & Bray,M. (2004) Pathogenesis of filoviral haemorrhagic fevers. Lancet Infectious Diseases, 4, 487-498

31 Martinez,O., Ndungo,E., Tantral,L., Miller,E.,H., Leung,L.,W., Chnadran,K., and Basler,C.,F. (2013) A Mutation in the Ebola Virus Envelope Glycoprotein Restricts Viral Entry in a Host Species- and Cell-Type-Specific Manner. Journal of Virology, 87, 3324-3334

32 Mateo,R., Nagamine,C.M., Spagnolo,J., Mendez,E., Rahe,M., Gale Jr,M., Yuan,J., Kirkegaard,K. (2013) Inhibition of Cellular Autophagy Deranges Dengue Virion Maturation. Journal of Virology, 87, 1312-1321

33 Mehedi,M., Falzarano,D., Seebach,J., Hu,X., Carpenter,M.S., Schnittler,H-j., and Feldmann,H. (2011) A new Ebola virus Nonstructural Glycoprotein Expressed through RNA Editing. Journal of Virology, 85, 5406-5414

34 Messaoudi,I., Amarasinghe,G.,K.,Basler,C.,F. (2015) Filovirus pathogenesis and immune evasion: insights from Ebola virus and Marburg virus. Nature Review Microbiology, 13, 663-676

35 Miranda,M.E., Ksiazek,T.G., Retuya,T.J., Khan,A.S., Sanchez,A., Fulhorst,C.F., Rollin,P.E., Calaor,A.B., Manalo,D.L., Roces,M.C. et al. (1999) Epidemiology of Ebola (Subtype Reston) Virus in the Philippines, 1996. Journal of Infectious Diseases, 179, Supplement1, S115-S119

36 Miranda,M.E.G. and Miranda,N.L.J. (2011) Reston ebolavirus in humans and animals in the Philippines: a review. Journal of Infectious Diseases, 204, Supplement3, S757-S760

37 Mizushima,N., Yoshimorim,T., Levine,B. (2010) Methods in Mammalian Autophagy Research. Cell, 140, 313-326

38 Nanbo,A., Imai,M., Watanabe,S., Noda,T., Takahashi,K., Neumann,G., Halfmann,P., and Kawaoka,Y. (2010) Ebolavirus is Internalized into Host Cells via Macropinocytosis in a Viral Glycoprotein-Dependent Manner. PLOS Pathogens,

39 Nezis,I. iLIR Autophagy Database. Available:https://ilir.warwick.ac.uk/index.php. Last accessed 2nd August 2018.

40 Nguyen,T,N., Padman,B,S., Usher,J., Oorschot,V., Ramm,G., Lazarou,M.(2016) Atg8 family LC3/GABARAP proteins are crucial for autophagosome-lysosome fusion but not autophagosome formation during

PINK1/Parkin mitophagy and starvation. Journal of Cell biology, 215, 857-874

41 Noda,T., Ebihara,H., Muramoto,Y., Fujii,K., Takada,A., Sagara,H., Kim,J.,H.,Kida,H., Feldmann,H., Kawaoka,Y. (2006) Assembly and Budding of Ebolavirus. PLOS Pathogens, 2, e99

42 Olejnik,J., Forero,A., Deflube,L.,R., Hume,A.,J., Manhart,W.,A., Nishida,A., Marzi,A., Katza,M.,G., Ebihara,H., et al (2017) Ebolaviruses Associated with Differential Pathogenicity Induce Distinct Host Responses in Human Macrophages. Journal of Virology, 91, e00179-17

43 Pappalardo,M., Julia,M., Howard,M.J., Rossman,J.S., Michaelis,M., and Wass,M.N. (2016) Conserved difference in protein sequence determine the human pathogenicity of Ebolaviruses. Scientific Reports, 6, 23743

44 Pratt,W.D., Wang,D., Nicholas,D.K., Luo,M., Woraratanadharm,J., Dye,J.M., Holman,D.H., and Dong,J.Y. (2010) Protection of Nonhuman Primates against Two Species of Ebola Virus Infection with a Single Complex Adenovirus Vector. Clinical and Vaccine Immunology, 17,572-581

45 Rhein,B.A., and Maury,W.J. (2015) Ebola Virus Entry into Host Cells: Identifying Therapeutic Strategies. Current Clinical Microbiology Reports, 2, 115-124

46 Sagnier,S., Daussy,C.F., Borel,S., Robert-Hebmann,V., Faure,M., Blanchet,F.P., Beaumelle,B., Biard-Piechaczyk,M., Espert,L. (2015) Autophagy Restricts HIV-1 Infection by Selectively Degrading Tat in CD4+ T Lymphocytes. Journal of Virology,89, 615-625

47 Sanchez,A., Kiley,M.P., Holloway,B.P., and Auperin,D.D. (1993) Sequence analysis of the Ebola virus genome:organization, genetic elements, and comparison with the genome of Marburg virus. Virus Research, 29, 215-240

48 Schudt,G., Dolnik,O., Kolesnikova,L., Biedenkopf,N., Herwig,A., and Becker,S. (2015) Transport of Ebolavirus Nucleocapsids is Dependent on Actin Polymerization: Live-Cell Imaging Analysis of Ebolavirus-Infected Cells. Journal of Infectious Diseases, 212, p S160-S166

49 Sharifi,M.,N.,Mowers,E.,E., Drake,L.,E., and Macleod,K.,F. (2015) Measuring Autophagy in Stressed Cells. Methods Mol Biol, 1292, 129-150

50 Shtanko,O., Reyes,A.,N., Jackson,W.,T., Davey,R.,A. (2018) Autophagy-Associated Proteins Control Ebola Virus Internalization Into Host Cells. Journal of Infectious Diseases, jiy294

51 Sparrer,K.M.J., and Gack,M.U. (2018) TRIM proteins: New players in virus-induced autophagy. PLOS Pathogens, 14,2,e1006787

52 Wang,M., and Jiang,S. (2015) Interaction between Autophagy and EBV: Impacts on the Autophagic Pathway and EBV Infection. International Journal of Bacterio-Virology, 1: 001

53 Watt,A., Moukambi,F., Banadyga,L., Groseth,A., CAllison,J., Herwig,A., Ebihara,H., Feldmann,H., Hoenen,T. (2014) A Novel Life cycle Modeling System for Ebola Virus Shows a Genome Length-Dependent Role of VP24 in Virus Infectivity. Journal of Virology, 88, 10511-10524

54 Wauquier,N., Becquart,P., Padilla,C., Baize,S., Leroy,E.M.(2010) Human Fatal Zaire Ebola Virus Infection is Associated with an Aberrant Innate Immunity and with Massive Lymphocyte Apoptosis. PLOS, 4, e837

55 Wong,A.S.L., Cheung,Z.H.,Ip.N.Y. (2011) Molecular Machinery of macroautophagy and its deregulation in diseases. Biochimica et Biophysica Acta, 1490-1497.

6 Supplementary data

6.1 EBOV LIR domains

Protein	Start	End	LIR sequence	PSSM Score	Pattern
zL	87	92	NGFCPV	4	WxxL
zL	150	155	FFWYDL	10	WxxL
zL	188	193	YVFWKI	0	WxxL
zL	268	273	PNFKIV	7	WxxL
zL	290	295	DGYKII	13	WxxL
zL	424	429	GSWYSV	13	WxxL
zL	446	451	NQFPPL	3	WxxL
zL	459	464	WEFYHL	5	WxxL
zL	492	497	TCWDAV	12	WxxL
zL	561	566	RTFGKL	7	WxxL
zL	671	676	QCYMHV	3	WxxL
zL	714	719	KLWTSI	13	WxxL
zL	828	833	AIFDDL	7	WxxL
zL	864	869	HTFFSV	4	WxxL
zL	872	877	LQYHHL	5	WxxL
zL	894	899	LDFGTI	10	WxxL
zL	920	925	CFYRNL	-2	WxxL
zL	947	952	DLFLPL	9	WxxL
zL	1084	1089	LWFSYL	1	WxxL
zL	1116	1121	YSWAHI	12	WxxL
zL	1162	1167	KPFVSV	7	WxxL
zL	1314	1319	IIFQNV	1	WxxL
zL	1457	1462	LTYPKI	6	WxxL
zL	1592	1597	FLYQIV	8	WxxL
zL	1763	1768	LPFFTL	4	WxxL
zL	1804	1809	CRFTGI	2	WxxL
zL	1853	1858	LFFNTL	2	WxxL
zL	1938	1943	KLYEAV	7	WxxL
zL	1999	2004	EWYLCL	5	WxxL
zL	2054	2059	LSYIRL	9	WxxL
zL	2070	2075	HRYNLV	2	WxxL
zL	2112	2117	QTYHFI	8	WxxL
zL	2132	2137	LKFFLI	4	WxxL
zL	2149	2154	AEFKKL	9	WxxL
zL	2162	2167	NRFYHI	3	WxxL

Protein	Start	End	LIR sequence	PSSM Score	Pattern
zNP	19	24	MDYHKI	10	WxxL
zNP	151	156	LSFASL	6	WxxL
zNP	189	194	TAWQSV	12	WxxL
zNP	210	215	IKFLLI	6	WxxL
zNP	239	244	ARFSGL	3	WxxL
zNP	294	299	APFARL	3	WxxL
zNP	311	316	GLFPQL	1	WxxL
zNP	338	343	EQYQQL	9	WxxL
zNP	650	655	EMYRHI	9	WxxL
zNP	660	665	GPFDAV	7	WxxL
zNP	710	715	NRFVTL	8	WxxL
zNP	719	724	QFYWPV	0	WxxL
zNP	729	734	NKFMAI	5	WxxL

Protein	Start	End	LIR sequence	PSSM Score	Pattern
zGP	18	23	SFFLWV	2	WxxL
zGP	160	165	FLYDRL	8	WxxL
zGP	181	186	VAFLIL	6	WxxL
zGP	239	244	LTYVQL	10	WxxL
zGP	306	311	LSFTVV	9	xLIR
zGP	580	585	RTFSIL	10	WxxL

Protein	Start	End	LIR sequence	PSSM Score	Pattern
zVP24	6	11	GRYNLI	5	WxxL
zVP24	40	45	VYWAGI	6	WxxL
zVP24	74	79	NLFPHL	1	WxxL
zVP24	170	175	VNYNGL	3	WxxL
zVP24	217	222	AKFSLL	6	WxxL

Protein	Start	End	LIR sequence	PSSM Score	Pattern
zVP30	209	214	EVYQRL	7	WxxL
zVP30	240	245	TAFLNI	4	WxxL

Protein	Start	End	LIR sequence	PSSM Score	Pattern
zVP35	42	47	DIFCDI	5	WxxL
zVP35	81	86	HSFEEV	9	WxxL
zVP35	140	145	AKYDLL	10	WxxL
zVP35	198	203	EAFNNL	3	WxxL
zVP35	227	232	IMYDHL	10	WxxL
zVP35	237	242	TAFHQL	2	WxxL
zVP35	322	327	RGWVCV	16	WxxL

Protein	Start	End	LIR sequence	PSSM Score	Pattern
zVP40	93	98	PIWLPL	13	WxxL
zVP40	245	250	QDFKIV	11	WxxL
zVP40	290	295	PKYIGL	7	WxxL

6.2 RESTV LIR domains

Protein	Start	End	LIR Sequence	PSSM Score	Pattern
rL	53	58	LKFDTI	9	WxxL
rL	150	155	FFWHDL	10	WxxL
rL	177	182	DEFIDI	14	xLIR
rL	188	193	YIFWKI	0	WxxL
rL	290	295	EGYKII	11	WxxL
rL	349	354	RDFHKI	12	WxxL
rL	363	368	QQFCEL	4	WxxL
rL	424	429	GTWYSV	13	WxxL
rL	446	451	NHFPSL	2	WxxL
rL	459	464	WEFYHL	5	WxxL
rL	492	497	TCWDAV	12	WxxL
rL	561	566	RTFGKL	7	WxxL
rL	671	676	QCYMHV	3	WxxL
rL	714	719	KLWTSI	13	WxxL
rL	828	833	AIFDDL	7	WxxL
rL	864	869	HTYFAV	5	WxxL
rL	872	877	LQYHHL	5	WxxL
rL	894	899	LDYGTI	11	WxxL
rL	947	952	DLFCPL	5	WxxL
rL	1084	1089	LWFSYL	1	WxxL
rL	1116	1121	YTWSHI	13	WxxL
rL	1160	1165	NAYVSV	7	WxxL
rL	1312	1317	IIFQNV	1	WxxL
rL	1412	1417	LRFPHL	2	WxxL

rL	1455	1460	LTYPQI	5	WxxL
rL	1464	1469	YSFGAV	3	WxxL
rL	1679	1684	EKYYNV	4	WxxL
rL	1761	1766	LPFFKL	3	WxxL
rL	1802	1807	CRFTGI	2	WxxL
rL	1936	1941	QLYRAV	2	WxxL
rL	1951	1956	PQYLKV	8	WxxL
rL	1997	2002	EWYLCL	5	WxxL
rL	2052	2057	CEYIGL	7	WxxL
rL	2068	2073	HRYNLV	2	WxxL
rL	2110	2115	QTYHFI	8	WxxL
rL	2130	2135	LKFSLI	5	WxxL
rL	2144	2149	SWYTEL	8	WxxL

Protein	Start	End	LIR Sequence	PSSM Score	Pattern
rNP	19	24	LDYHKI	11	WxxL
rNP	151	156	LSFASL	6	WxxL
rNP	189	194	TAWQSV	12	WxxL
rNP	210	215	IKYLLI	7	WxxL
rNP	239	244	ARFSGL	3	WxxL
rNP	294	299	APFARL	3	WxxL
rNP	311	316	GLYPQL	2	WxxL
rNP	338	343	EQYQQL	9	WxxL
rNP	599	604	PDYTAV	14	xLIR
rNP	650	655	ETYHHL	9	WxxL
rNP	660	665	GPFEAI	8	WxxL
rNP	710	715	NRYIYI	8	WxxL
rNP	719	724	QFFWPV	-1	WxxL
rNP	729	734	DKFLAI	11	WxxL

Protein	Start	End	LIR Sequence	PSSM Score	Pattern
rGP	3	8	SGYQLL	12	xLIR
rGP	21	26	LVWVII	14	xLIR
rGP	161	166	FLYDRL	8	WxxL
rGP	182	187	VAFLIL	6	WxxL
rGP	212	217	SYYMTL	7	WxxL
rGP	240	245	HTYVQL	9	WxxL
rGP	307	312	LHFQIL	7	WxxL
rGP	517	522	YYWTAV	10	WxxL
rGP	581	586	RTYSLL	10	WxxL

Protein	Start	End	LIR Sequence	PSSM Score	Pattern
rVP24	6	11	GRYNLV	4	WxxL
rVP24	21	26	VIFSDL	2	WxxL
rVP24	40	45	VYWAGI	6	WxxL
rVP24	74	79	NLFPHL	1	WxxL
rVP24	170	175	VNYNGL	3	WxxL
rVP24	217	222	VKFSLL	4	WxxL
rVP24	228	233	KPFTRV	5	WxxL
rVP24	243	248	MEFNSL	6	WxxL

Protein	Start	End	LIR Sequence	PSSM Score	Pattern
rVP30	209	214	EVYQRL	7	WxxL
rVP30	240	245	SAFLNI	6	WxxL

Protein	Start	End	LIR Sequence	PSSM Score	Pattern
rVP35	31	36	DIFIDI	9	WxxL
rVP35	66	71	VNYVPL	9	WxxL
rVP35	129	134	AKYDLL	10	WxxL
rVP35	187	192	EAYKNL	5	WxxL
rVP35	216	221	IMYDHL	10	WxxL
rVP35	226	231	TAFHQL	2	WxxL
rVP35	274	279	PIFQDV	5	WxxL
rVP35	311	316	RGWVCL	17	WxxL

Protein	Start	End	LIR Sequence	PSSM Score	Pattern
rVP40	93	98	PIWLPL	13	WxxL
rVP40	123	128	THFGKI	2	WxxL
rVP40	290	295	PKYVGL	8	WxxL

6.3 zNP and zVP35 previously seen to activate autophagy

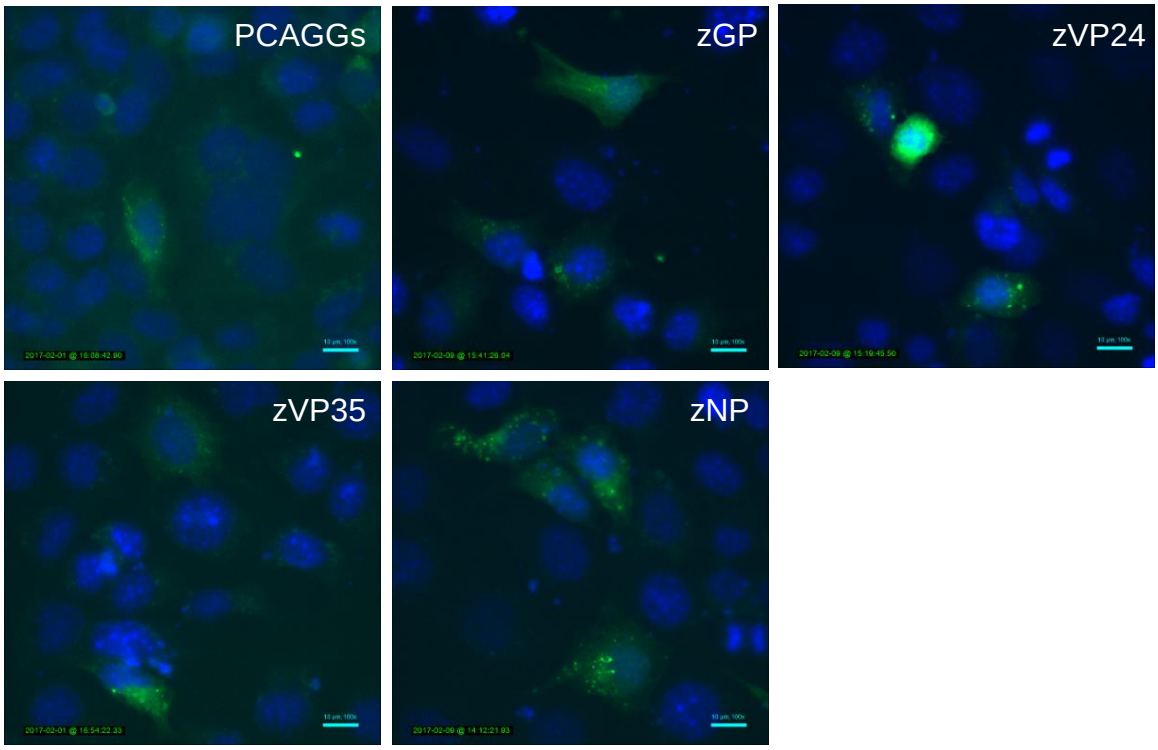

MEF cells were transfected with individual EBOV proteins, as indicated besides the images, and GFP-LC3. Activation of autophagy is seen by the formation of LC3 puncta. LC3 puncta can be seen as bright green dots, or aggregations. All slides were fixed at 24hrs post transfection and analysed by fluorescence microscopy. Nuclei are stained blue by DAPI.